

**Paper 4 open access : Effect of sonication time on the thermal stability, moisture absorption, and biodegradation of water hyacinth (*Eichhornia crassipes*) nanocellulose-filled bengkuang (*Pachyrhizus erosus*) starch biocomposites**

<https://www.sciencedirect.com/science/article/pii/S2238785419306635>

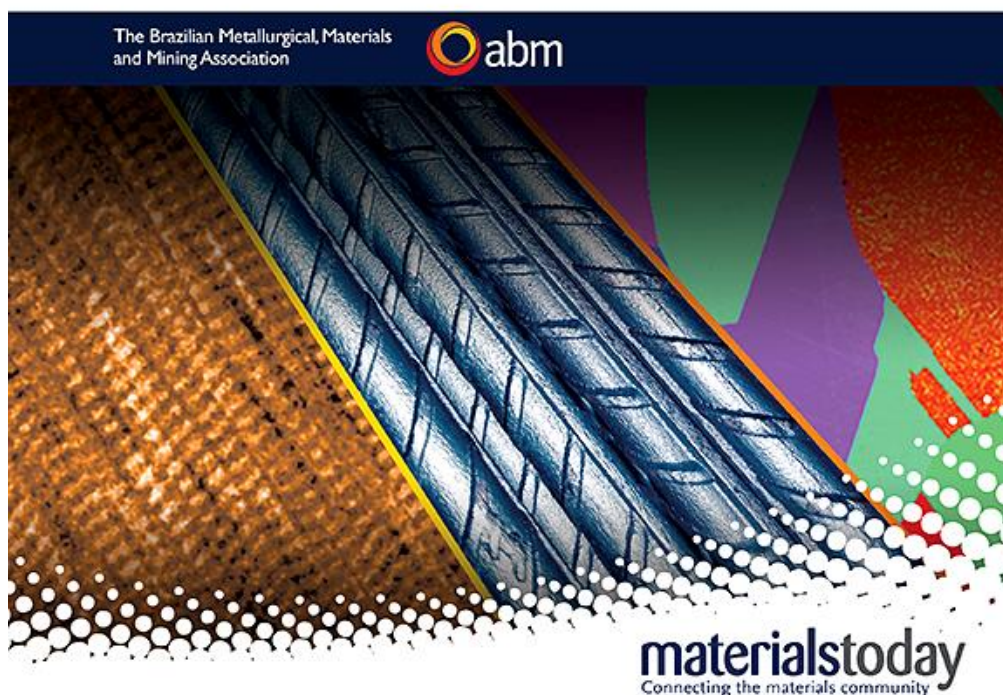
Full Paper dapat dilihat di bagian bawah



ISSN 2238-7854

# JMR&T

JOURNAL OF MATERIALS  
RESEARCH AND TECHNOLOGY





Original Article

# Effect of sonication time on the thermal stability, moisture absorption, and biodegradation of water hyacinth (*Eichhornia crassipes*) nanocellulose-filled bengkuang (*Pachyrhizus erosus*) starch biocomposites

Edi Syafri<sup>a</sup>  , Sudirman<sup>b</sup>, Mashadi<sup>b</sup>, Evi Yulianti<sup>b</sup>, Deswita<sup>b</sup>, Mochamad Asrofi<sup>c</sup>, Hairul Abrial<sup>d</sup>, S.M. Sapuan<sup>e,f</sup>, R.A. Ilyas<sup>e,f</sup>, Ahmad Fudholi<sup>g</sup>  

## Editorial Board

### Editor-in-Chief

**Marc André Meyers**

University of California, USA

### Associate Editors

**Carlos Hoffmann Sampaio**

Polytechnic University of Catalonia, Barcelona, Spain

**Dilson Silva dos Santos**

Universidade Federal do Rio de Janeiro, Brazil

**Lawrence E. Murr**

University of Texas at El Paso, USA

**Marcelo Breda Mourão**

Universidade de São Paulo, Brazil

**Paulo Rangel Rios**

Universidade Federal Fluminense, Brazil

**Ronaldo Barbosa**

Universidade Federal de Minas Gerais, Brazil

**Ruslan Z. Valiev**

Ufa State Aviation Technical University, Russia

**Sergio Neves Monteiro**

Instituto Militar de Engenharia, Brazil

**Po-Yu Chen**

National Tsing Hua University, Taiwan

**Qi Li**

Institute of Metal Research, Chinese Academy of Sciences, China

**Terence G. Langdon**

University of Southampton, UK

### Managing Editor

**Wen Yang**

USA

### Advisory Board

**Achilles Junqueira Bourdot Dutra**

Universidade Federal do Rio de Janeiro, Brazil

**Akihisa Inoue**

Tohoku University, Japan

**Amauri Garcia**

Universidade Estadual de Campinas, Brazil

**André Costa e Silva**

Universidade Federal Fluminense, Brazil

**Antônio Cezar Faria Vilela**

Universidade Federal do Rio Grande do Sul, Brazil

**Arthur Pinto Chaves**

Universidade de São Paulo, Brazil

**Claudemiro Bolfarini**

Universidade Federal de São Carlos, Brazil

**Claudio Shyinti Kiminami**

Universidade Federal de São Carlos, Brazil

**Dierk Raabe**

Max Planck Institut für Eisenforschung, Germany

**Enrique Lavernia**

University of California, USA

**Fathi Habashi**

Université Laval, Canada

**Hael Mughrabi**

Universität Erlangen, Germany

**Harshad Kumar Dharamshi Bhadeshia**

University of Cambridge, UK

**Ivan Gilberto Sandoval Falleiros**

Universidade de São Paulo, Brazil

**Jader Furtado**

Air Liquide R&D, Jouy-en-Josas Cedex, France

**Jun-ichiro Yagi**

Tohoku University, Japan

**Ke Lu**

Chinese Academy of Sciences, China

**Norbert Huber**

Helmholtz-Zentrum Geesthacht, Germany

**Olgun Güven**

Hacettepe University, Turkey

**Paulo Antonio de Souza Jr.**

The Commonwealth Scientific and Industrial Research Organization), Australia

**Pedro Dolabella Portella**

BAM, Federal Institute for Materials Testing, Germany

**Rubens Caram**

Universidade Estadual de Campinas, Brazil

**Stephen Liu**

Colorado School of Mines, USA

**Thaddeus Massalski**

Carnegie Mellon University, USA

**Victor Carlos Pandolfelli**

Universidade Federal de São Carlos, Brazil

**Virginia Sampaio Teixeira Ciminelli**

Universidade Federal de Minas Gerais, Brazil

**Xiang Zhang**

Cranfield University, UK

Scopus Preview

Journal of Materials Research and Technology

Open Access

Scopus coverage years: from 2012 to Present

Publisher: Elsevier

E-ISSN: 2238-7854

Subject area: [Materials Science: Metals and Alloys](#) [Materials Science: Surfaces, Coatings and Films](#) [Materials Science: Ceramics and Composites](#) [Materials Science: Biomaterials](#)

Source type: Journal

CiteScore 2021: 5.9

SJR 2021: 0.964

SNIP 2021: 1.672

View all documents | Set document alert | Save to source list | Source Homepage

CiteScore CiteScore rank & trend Scopus content coverage

Improved CiteScore methodology

CiteScore 2021 counts the citations received in 2018-2021 to articles, reviews, conference papers, book chapters and data

Journal of Materials Research and Technology

COUNTRY	SUBJECT AREA AND CATEGORY	PUBLISHER	H-INDEX
Brazil	Materials Science Biomaterials Ceramics and Composites Metals and Alloys Surfaces, Coatings and Films	Elsevier Editora Ltda	59
Universities and research institutions in Brazil			
Media Ranking in Brazil			
PUBLICATION TYPE	ISSN	COVERAGE	INFORMATION
Journals	22387854	2012-2021	Homepage How to publish in this journal

Improving the stability | Scopus preview - Sci | Journal of Materials R | (25) WhatsApp | SEM GANJIL 2019-20 | Journal of Materials R | SK Dosen Pengasuh |

scimagojr.com/journalsearch.php?q=21100383742&tip=sid&clean=0

Gmail Maps YouTube Gmail Edi Syafri - YouTube News

**% International Collaboration**

Year	% International Collaboration
2012	15
2013	25
2014	15
2015	18
2016	25
2017	20
2018	18
2019	25
2020	35

**Citable documents** **Non-citable documents**

Year	Citable documents	Non-citable documents
2012	0	0
2013	0	0
2014	0	0
2015	0	0
2016	0	0
2017	0	0
2018	0	0
2019	1000	0
2020	2500	0

**Cited documents** **Uncited documents**

Year	Cited documents	Uncited documents
2012	0	0
2013	0	0
2014	0	0
2015	0	0
2016	0	0
2017	0	0
2018	0	0
2019	1000	0
2020	2500	0

**Journal of Materials Research and Technology**

← Show this widget in your own website

Just copy the code below and paste within your html code:

```
<a href="https://www.scimagojr.com" >
```

Q1 Ceramics and Composites best quartile

SJR 2021 0.96

powered by scimagojr.com

**SCImago Graphica**

Explore, visually communicate and make sense of data with our **new data visualization tool**.

**S&P Global Market Intelligence** **Don't just make sustainability progress. Measure it.** **Seek & Prosper Align your impact >**

Type here to search | 25°C Hujan ringan | 13:20 09/04/2023

## List of Contents

Volume 8, Issue 6, November–December 2019, Pages 6223-6231

<https://www.sciencedirect.com/science/article/pii/S2238785419306635>

Research article Open access

**Effect of sonication time on the thermal stability, moisture absorption, and biodegradation of water hyacinth (*Eichhornia crassipes*) nanocellulose-filled bengkuang (*Pachyrhizus erosus*) starch biocomposites**

Edi Syafri, Sudirman, Mashadi, Evi Yulianti, ... Ahmad Fudholi

Pages 6223-6231

[View PDF](#)

Investigation of microstructure and texture during continuous bending of rolled AZ31 sheet by experiment and FEM

Fangkun Ning, Xiong Zhou, Qichi Le, Xiaoqiang Li, ... Weitao Jia

Pages 6232-6243

[View PDF](#)

Minimizing of copper losses to converter slag by a boron compound addition

Mehmet Ali Topçu, Aydın Rüßen, Bora Derin

Pages 6244-6252

[View PDF](#)

Characterization of geopolymers prepared using powdered brick

Jan Fořt, Radimír Novotný, Eva Vejmelková, Anton Trník, ... Robert Černý

Pages 6253-6261

[View PDF](#)

Effect of the carbon loading on the structural and photocatalytic properties of reduced graphene oxide-TiO<sub>2</sub> nanocomposites prepared by hydrothermal synthesis

Bruno S. Gonçalves, Hugo G. Palhares, Tarcizo C.C. de Souza, Vinícius G. de Castro, ... Eduardo H.M. Nunes

Pages 6262-6274

[View PDF](#)

Microstructure and crystallographic orientation evolutions below the superficial white layer of a used pearlitic rail

Mohammad Masoumi, Nelson Batista de Lima, Gustavo Tressia, Amilton Sinatora, Hélio Goldenstein

Pages 6275-6288

[View PDF](#)

Enhanced interfacial strength of carbon fiber/PEEK composites using a facile approach via PEI&ZIF-67 synergistic modification

Hansong Liu, Yan Zhao, Na Li, Xiaoran Zhao, ... Shanyi Du

Pages 6289-6300

[View PDF](#)

Article preview

Structural analysis of Al–Ce compound phase in AZ-Ce cast magnesium alloy

Su Juan, Guo Feng, Cai Huisheng, Liu Liang

Pages 6301-6307

[View PDF](#)

A review on relationship between morphology of boride of Fe-B alloys and the wear/corrosion resistant properties and mechanisms

Jianjun Zhang, Jiachen Liu, Huimin Liao, Ming Zeng, Sude Ma

Pages 6308-6320

[View PDF](#)

Available online at [www.sciencedirect.com](http://www.sciencedirect.com)

**jmr&t**  
Journal of Materials Research and Technology  
[www.jmrt.com.br](http://www.jmrt.com.br)



## Original Article

# Effect of sonication time on the thermal stability, moisture absorption, and biodegradation of water hyacinth (*Eichhornia crassipes*) nanocellulose-filled bengkuang (*Pachyrhizus erosus*) starch biocomposites



Edi Syafri<sup>a,\*</sup>, Sudirman<sup>b</sup>, Mashadi<sup>b</sup>, Evi Yulianti<sup>b</sup>, Deswita<sup>b</sup>, Mochamad Asrofi<sup>c</sup>, Hairul Abral<sup>d</sup>, S.M. Sapuan<sup>e,f</sup>, R.A. Ilyas<sup>e,f</sup>, Ahmad Fudholi<sup>g,\*</sup>

<sup>a</sup> Department of Agricultural Technology, Agricultural Polytechnic, Payakumbuh, West Sumatra 26271, Indonesia

<sup>b</sup> Center for Science and Technology of Advanced Materials, National Nuclear Energy Agency, Kawasan Nuklir, PUSPITEK Serpong, Banten, Indonesia

<sup>c</sup> Laboratory of Material Testing, Department of Mechanical Engineering, University of Jember, Kampus Tegalboto, Jember 68121, East Java, Indonesia

<sup>d</sup> Department of Mechanical Engineering, Andalas University, Kampus Limau Manis, Pauh, Padang 25163, Indonesia

<sup>e</sup> Laboratory of Biocomposite Technology, Institute of Tropical Forestry and Forest Products, Universiti Putra Malaysia, Serdang 43400, Selangor, Malaysia

<sup>f</sup> Department of Mechanical and Manufacturing Engineering, Universiti Putra Malaysia, Serdang 43400, Selangor, Malaysia

<sup>g</sup> Solar Energy Research Institute, Universiti Kebangsaan Malaysia, 43600 Bangi, Selangor, Malaysia

## ARTICLE INFO

## Article history:

Received 23 May 2019

Accepted 8 October 2019

Available online 13 November 2019

## Keywords:

Nanocellulose

Biodegradation

Biocomposites

Hyacinth fiber

Thermogravimetric analysis

## ABSTRACT

In Indonesia, starch, particularly that obtained from bengkuang (*Pachyrhizus erosus*), is abundant and inexpensive, thereby increasing the value of bengkuang starch, which can be mixed with bioplastic-based starch. A biocomposite comprising nanocellulose from water hyacinth (*Eichhornia crassipes*) and bengkuang starch was successfully fabricated using the solution casting method. Nanocellulose content in the matrix was kept constant at 1 wt%. Moreover, during fabrication, the biocomposite gel was treated in an ultrasonic bath for 0, 15, 30, and 60 min. Further, thermogravimetric analysis, moisture absorption measurements, Fourier transform infrared spectroscopy, and scanning electron microscopy were performed. The biocomposite sample vibrated for 60 min had the highest thermal stability and exhibited low moisture absorption. The soil burial test proved that this biocomposite, as opposed to 0-min vibrated samples, has a slower biodegradation rate. This result was supported by morphological evaluation after biodegradation, in which the 60-min vibrated samples showed a coarse surface and low porosity formation.

© 2019 The Authors. Published by Elsevier B.V. This is an open access article under the CC BY-NC-ND license (<http://creativecommons.org/licenses/by-nc-nd/4.0/>).

\* Corresponding author.

E-mails: [edi.syafri@politanipyk.ac.id](mailto:edi.syafri@politanipyk.ac.id) (E. Syafri), [a.fudholi@ukm.edu.my](mailto:a.fudholi@ukm.edu.my) (A. Fudholi).

<https://doi.org/10.1016/j.jmrt.2019.10.016>

2238-7854/© 2019 The Authors. Published by Elsevier B.V. This is an open access article under the CC BY-NC-ND license (<http://creativecommons.org/licenses/by-nc-nd/4.0/>).

## 1. Introduction

Plastic is widely used in many applications, including its use in food packaging, electronic components, and automotive dashboards. Usually, plastic is made using crude oil. However, plastic has a negative impact on the environment because it is nondegradable and it causes air pollution [1]. In 2010, Indonesia was responsible for the second highest level of marine plastic pollution after China. The total production of marine plastic debris globally ranges 0.48–1.29 million metric tons per year [2].

One breakthrough solution to this problem was the development of biodegradable plastic (bioplastic). Generally, bioplastic comprises starch, polylactic acid, and polyvinyl alcohol. In Indonesia, starch, especially that from bengkung (*Pachyrhizus erosus*), is abundant and inexpensive [3–5]. The total production of bengkung has reached 191.5 quintals/ha per year, thereby indirectly increasing the value of bengkung starch based on its ability to be mixed with bioplastic-based starch. Bengkulu starch has several advantages, namely its availability, low cost, and environmental friendliness. This starch has a high amylose content of approximately 30%–40% [6,7]. However, this starch has the disadvantages of low thermal stability and high moisture absorption [7]. The addition of cellulose fiber is an alternative solution to such problems.

Cellulose fiber from water hyacinth (*Eichhornia crassipes*) is a candidate for reinforcement because of its high cellulose content and abundance in nature [8,9]. Water hyacinth is a free-floating macrophyte that exhibits a fast growth rate, adaptability to a wide range of environmental conditions, and high nutrient uptake capacity. Cellulose in the nanometer range, called nanocellulose, has become prevalent in recent years. Nanocellulose has several advantages, such as being biodegradable and renewable and having acceptable transparency [10,11]. Prior research established that the addition of nanocellulose in the matrix increased thermal and moisture resistance.

However, these properties depend on several factors, including porosity, the agglomeration phenomenon, and the dispersion of nanocellulose in the matrix [12]. Ultrasonication is used to reduce the formation of agglomeration and increase the dispersity of nanocellulose in fibers. Several studies reported the use of ultrasonic treatment of nanocellulose for reducing agglomeration during gelatinization. Previous researchers prepared and sonicated biocomposites from cellulose fiber-reinforced starch during gelatinization using an ultrasonic bath instrument. They claimed that sonication successfully reduced fiber agglomeration in the starch matrix [12,13]. However, their work did not reveal the biodegradation characteristic of the biocomposite sample. Note that biodegradation has an important role in biocomposites, as previously reported [14,15].

Several researchers have investigated the use of distilled water to clean samples after biodegradation in soil [14,15]. However, this method is ineffective for separating soil from samples. Soil continues to adhere to samples because of the lowest-energy water, as substantiated by several experiments. Accordingly, this work proposed a new method for

cleaning samples. Using an ultrasonic bath is an effective means of separating soil from samples after biodegradation. The morphological characteristics of samples after biodegradation were observed via scanning electron microscopy (SEM). Thermogravimetric analysis (TGA), moisture absorption measurements, and Fourier transform infrared (FTIR) spectrometry were conducted to determine thermal stability, moisture resistance, and the functional group of the biocomposites, respectively. This study aimed to investigate the effect of the vibration (sonication) duration (0, 15, 30, or 60 min) during the fabrication of biocomposite samples, specifically focusing on thermal stability, moisture resistance, and biodegradation in soil.

## 2. Materials and methods

### 2.1. Materials

Water hyacinth fiber was obtained from Payakumbuh, Indonesia. Nanocellulose was obtained from water hyacinth fiber via chemical and mechanical treatment. The lignin, hemicellulose, and cellulose contents of water hyacinth were 7%, 29%, and 43%, respectively. Bengkulu tubers were purchased from local farmers in Kuranji, Padang, Indonesia. All chemical reagents, such as distilled water, glycerol, NaOH, NaClO<sub>2</sub>, CH<sub>3</sub>COOH, and HCl, were obtained from the Metallurgy Mechanic Laboratory, Andalas University.

### 2.2. Extraction of bengkung starch

Bengkung tubers were peeled, cut into small pieces, and then crushed using an ice blender at 10,000 rpm for 5 min to obtain the resulting porridge. The porridge was filtered using a mesh screen (200 mesh) to separate the bagasse and suspension. Furthermore, the suspension was precipitated for 5 h to acquire the bengkung starch. The precipitant was dried in an oven at 50 °C for 20 h. Then, the resulting material was collected and crushed to produce dry starch powder.

### 2.3. Isolation of nanocellulose from water hyacinth

Water hyacinth fiber was prepared as previously described [9]. Dried water hyacinth fiber (15 g) was pulped using 15% sodium hydroxide solution. The mixture was heated and stirred at 60 °C and 300 rpm for 4 h. Then, the fiber was cleaned from the alkali solution with distilled water. Bleaching was performed using sodium chlorite and acetic acid (4:1). This process was conducted at 60 °C and 300 rpm for 2 h. The mixture was rinsed with distilled water to obtain the cellulose suspension. Next, 5 M HCl was added to the suspension for acid hydrolysis at 60 °C and 300 rpm for 20 h. HCl was used to isolate nanocellulose from the cellulose fiber. Then, the products were neutralized using distilled water before ultrasonication. An ultrasonic crusher was utilized to produce nanocellulose from water hyacinth. This process was conducted at 600 W for 1 h.

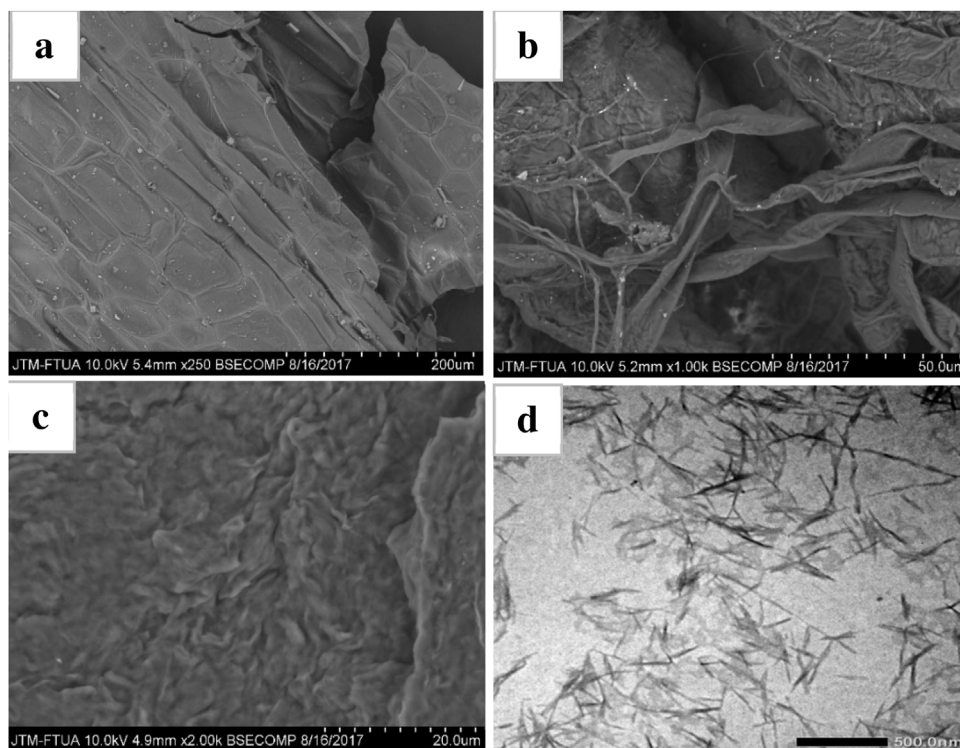


**Fig. 1 – Water hyacinth fiber before and after treatment. (a) Raw fiber (untreated), (b) bleached fiber, (c) fiber subjected to acid hydrolysis; and (d) fiber subjected to ultrasonication.**

#### 2.4. Biocomposite fabrication

A total of 10 g of bengkuang starch was mixed with 100 ml of distilled water in a glass beaker. This mixture was homogenized using an ultrasonic homogenizer at 8000 rpm for 5 min. During homogenization, 1% NWHF and 2 ml of glycerol were slowly added to the mixing solution. A constant fraction of nanocellulose (1 wt%) was used as reinforcement in the bengkuang starch matrix. Then, the mixing solution was heated and stirred at 60 °C and 500 rpm for 30 min (until gelatinized). The biocomposite gel (70 g) was poured in a Petri dish (15 cm diameter). The gel was incubated in an ultrasonic bath for 0, 15, 30, or 60 min and labeled as VT 0 (untreated), VT 15, VT 30, and VT 60, respectively. Subsequently, the biocomposite was dried in a drying oven at 50 °C for 20 h.

#### 2.5. Characterization

##### 2.5.1. SEM

The morphology of the untreated and treated water hyacinth fibers as well as the morphological characteristic of all biocomposites tested after biodegradation in soil were observed using a Hitachi 3400 N scanning electron microscope. The operation voltage was 10 kV. The fracture surface of the biocomposite was studied through a VEGA3 TESCAN SEM instrument at room temperature and 10 kV. All samples were coated with gold using an argon plasma metalizer (sputter coater K575X, Edwards Limited, Crawley, UK) to avoid charging.

##### 2.5.2. Transmission electron microscopy (TEM)

A JEM-JEOL 1400 TEM instrument was operated at 100 keV to observe the nanocellulose fibers. The nanocellulose suspension was cast in a carbon-coated grid and then directly observed at room temperature.

##### 2.5.3. Thermogravimetric analysis

All samples were tested using a TGA/DTG 60 system (serial no. C30565000570) to determine the thermal degradation point at each stage. The test was conducted over the temperature range of 30 °C–550 °C under a nitrogen atmosphere. The heating rate was maintained at 10 °C/min. The weight of all tested samples was 5–7 mg.

##### 2.5.4. Moisture absorption

All tested samples were cut into 1 cm × 3 cm pieces and dried in a drying oven to a constant weight. The initial ( $W_0$ ) and final weights ( $W_t$ ) were recorded. Moisture absorption was examined in a moisture chamber (relative humidity [RH]: 75%) at 25 °C. The percent moisture absorption was calculated using the following equation [12]:

$$\text{Moisture Absorption} = \frac{W_t - W_0}{W_0} \times 100\%. \quad (1)$$

##### 2.5.5. FTIR spectroscopy

FTIR spectroscopy was used to determine the functional groups of all samples. The FTIR spectrum of all tested samples was recorded using a Perkin-Elmer Frontier FTIR instrument

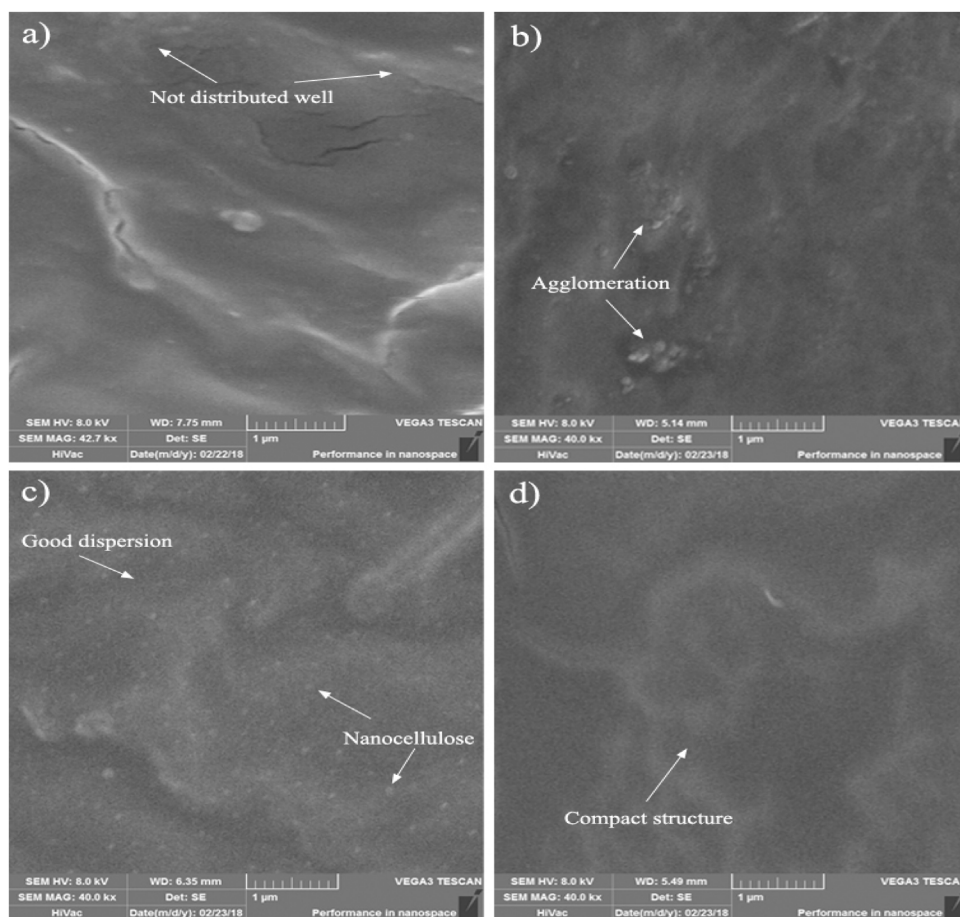


**Fig. 2 – Fracture surface of all biocomposite samples. Samples were vibrated for (a) 0, (b) 15, (c) 30, or (d) 60 min.**

with a resolution of  $4\text{ cm}^{-1}$ . The scanned wavenumber range was  $600\text{--}4000\text{ cm}^{-1}$ .

### 2.5.6. Soil burial test

The biodegradation test was conducted by burying the samples in soil that was purchased from PT. Mahesa Mutiara Tani (Kompos Nesia, Bogor, Indonesia). The soil contained organic carbon (34.25%), nitrogen (2%), ferrous (7.9%), pH (7.33), diphosphorus pentoxide (0.62%), other materials (e.g., plastic, glass, gravel = 0.1%), and several colonies in 1 g of soil ( $8 \times 10^{14}$  CFU), and its carbon-to-nitrogen ratio was 17.15%.

**Control sample:** The sample was cut into  $10\text{ mm} \times 10\text{ mm}$  pieces and then dried in a drying oven at  $50^\circ\text{C}$  for 20 h to a constant weight. Then, the sample was subjected to ultrasonic bath treatment for 5 min and dried in an oven at  $50^\circ\text{C}$  for 20 h. Subsequently, the sample was weighed using a precision balance (accuracy = 0.001). The weight loss of the control sample was calculated as the difference between  $W_0$  before ultrasonic bath treatment and  $W_t$  after the treatment.

**Buried samples:** All samples for the burial test measured  $10\text{ mm} \times 10\text{ mm}$ . The samples were dried in a drying oven at  $50^\circ\text{C}$  for 20 h to a constant weight and weighed using a precision balance to obtain  $W_0$  before burial in soil. Then, the test was conducted in a square container ( $10\text{ cm} \times 10\text{ cm}$ ) containing soil an RH and temperature of 60%–65% and  $25^\circ\text{C}$ ,

respectively. After vibration, biodegradation was observed after 3, 7, and 15 days of burial in soil.

After burial, all samples were collected and cleaned using a paintbrush. Then, the samples were subjected to ultrasonic bath treatment for 5 min to remove the soil that adhered to the biocomposites. The samples were dried in a drying oven at  $50^\circ\text{C}$  for 20 h to a constant weight. Afterward, they were weighed using an analytical balance. The percent weight loss of the sample due to soil burial was calculated according to the different weights before and after the burial test. The percent weight loss due to soil was calculated using the following equation:

$$W_{\text{degradation}} = W_{\text{burial test}} - W_{\text{control}} \quad (2)$$

## 3. Results and discussion

### 3.1. Morphological characteristics of untreated and treated fibers

Fig. 1 shows the morphological features of water hyacinth fiber before and after treatment. Fig. 1a displays the raw water hyacinth fiber (untreated), which had a smooth surface, and some microfibrils were still bound. Untreated fiber contains lignin substances such as waxes and oils [16,17]. Bleaching

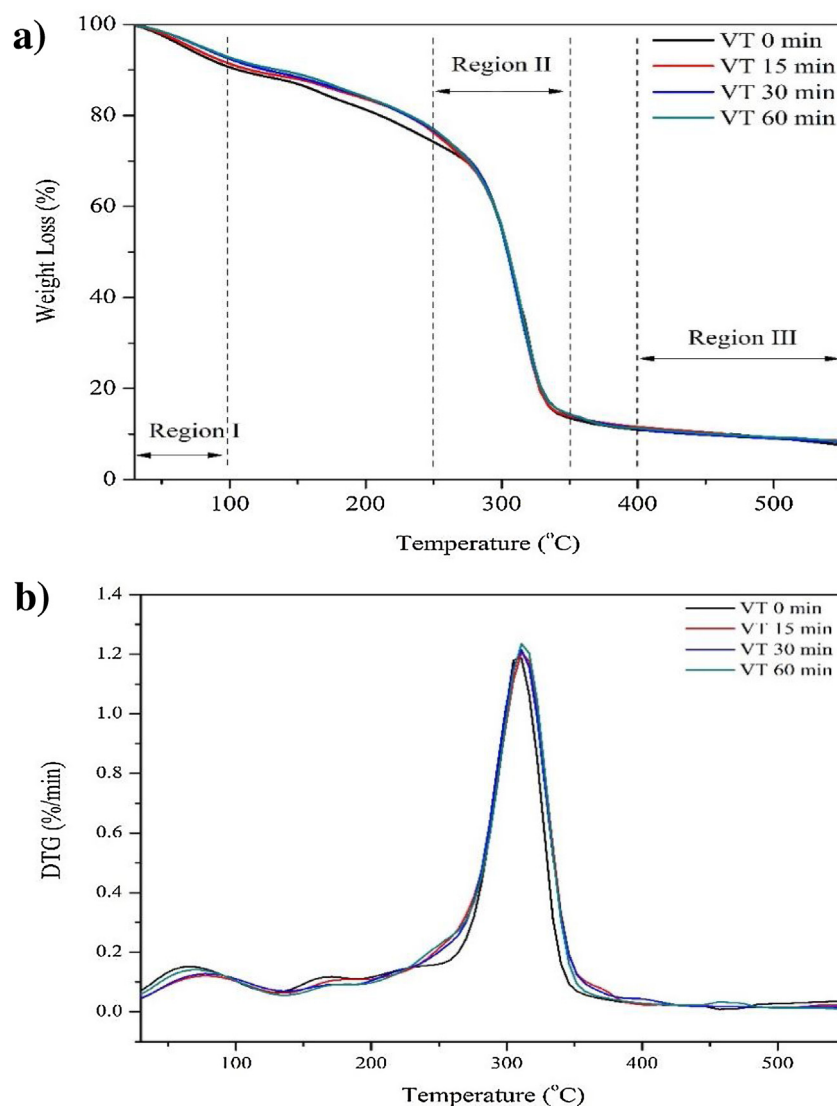


**Fig. 3 – (a) Thermogravimetric analysis and (b) DTG curves of all biocomposite samples.**

successfully destroyed several microfibril bonds, as presented in Fig. 1b, because of the broken linkage between lignin and hemicellulose. A similar phenomenon was reported by a previous study [9,18]. In the acid hydrolysis process (Fig. 1c), the fiber was depolymerized into short individual microfibrils with a diameter and length of 2 and 6 microns, respectively. Nanocellulose was obtained via ultrasonication for 1 h. Fig. 1d displays the distribution of cellulose fibers in the nanometer range. Cellulose fibers were dispersed homogeneously, as shown in the TEM images (Fig. 1d), measuring 15 nm in diameter and 147 nm in length. This outcome is attributable to the high intensity of the power ultrasound, resulting in short cellulose fibers in the nanometer range [19,20].

### 3.2. Fracture surface of the biocomposites

Fig. 2 shows the fracture surface of untreated and treated biocomposite films. Fig. 2a displays the fracture morphology of the VT 0 min sample (untreated). The cellulose fibers in bengkuan starch were not distributed well. Thus, the mixing

of starch and cellulose was not homogeneous during fabrication [21]. This explained the low thermal stability of the untreated biocomposite. A poor distribution of nanocellulose affects thermal stability in terms of interfacial adhesion between the nanocellulose and starch biopolymers. That is, the strong interfacial adhesion between nanocellulose and starch corresponded to the high thermal stability of the biocomposites because a high temperature is required to break the bonds between nanocellulose and starch biopolymers.

The VT 15 min sample also exhibited no significant fracture morphology. The agglomeration phenomenon remains apparent in this sample (Fig. 2b). According to a previous report, agglomeration and poor dispersion of cellulose fibers lead to decreased thermal and moisture resistance [22]. The different fracture morphologies are shown in Fig. 2c and d for the VT 30 min and VT 60 min samples, respectively. In these cases, the samples displayed good dispersion and compact structures. These findings are probably attributable to the kinetic energy from the ultrasonic bath, leading to improved interfacial bonding between the fibers and matrix [12,13]. This

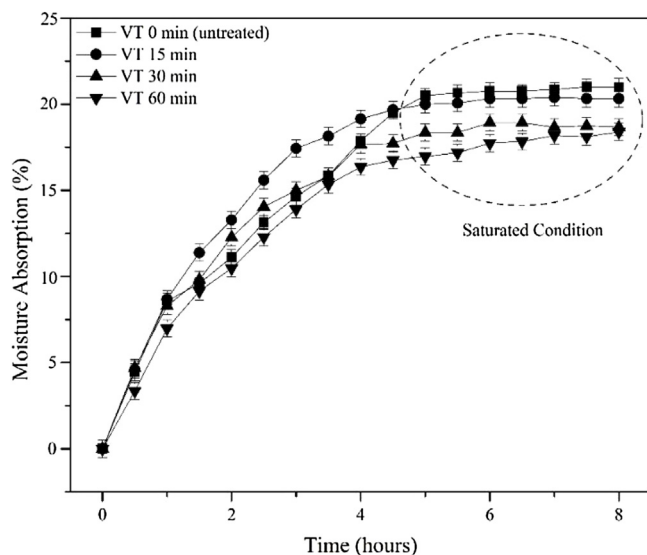


**Fig. 4 – Moisture absorption of all tested biocomposite samples. Samples were subjected to ultrasonication for 0, 15, 30, or 60 min. VT: vibration time.**

treatment also resulted in good dispersion of the nanocellulose in the matrix and reduced the free OH bonding between the fibers and matrix. This phenomenon was similar to that observed by Asrofi et al. [6] concerning the effect of ultrasonic vibration during processing on the mechanical properties of a water hyacinth nanofiber cellulose-reinforced thermoplastic starch bionanocomposite.

### 3.3. Thermal stability

The thermal characteristics of the biocomposite samples with various vibration times were presented using TGA (Fig. 3a) and DTG (Fig. 3b) curves. Two main degradation areas were found in accordance with the results from previous research [23–25]. The first region of degradation reflected the initial degradation of all biocomposite samples at temperatures of less than 100 °C as indicated by the TGA and DTG curves. This result revealed increasing weight loss compared with  $W_0$  before testing. The percent weight loss values of the biocomposite in the first region were 11% (VT 0 min), 9% (VT 15 min), 9% (VT 30 min), and 7% (VT 60 min). This phenomenon was attributable to the moisture content in all samples [8,25]. These results were supported by the DTG curve (Fig. 1b), which reveals the presence of small peaks in the temperature range of 50 °C–100 °C.

The second region (250 °C–350 °C) involved significant weight loss exceeding 50% for all samples. In this condition, the structures of starch, glycerol, and nanocellulose fibers were degraded [12,26]. The DTG curve (Fig. 1b) exhibits a sharp peak due to the significant weight reduction. The degradation temperatures for all samples in this area was 305 °C, 309 °C, 311 °C, and 318 °C for VT 0, VT 15, VT 30, and VT 60 min, respectively. Untreated biocomposite samples (VT 0) min had lower degradation temperatures. This outcome indicated fiber agglomerated and porosity formation in the matrix that resulted in reduced thermal stability [4]. Thermal stability

and moisture resistance increased with prolonged ultrasonic vibration.

Conversely, increased vibration time improved the thermal stability of the biocomposite samples. This result was supported by the increase in the degradation temperature of the treated samples compared with that of the untreated sample due to the improved interfacial adhesion between the fibers and matrix as a result of the kinetic energy of the ultrasonic bath. Good adhesion was indicated by the scarcity of free OH between the fibers and matrix [6,8,12].

In the third region (>400 °C), all samples were completely decomposed, becoming ash [25,26]. However, the treated samples had higher thermal stability than untreated samples because of the kinetic energy of the ultrasonic bath, which allowed the fibers to disperse evenly in the matrix. Other effects of the bath included good dispersion of the fibers in the matrix, a compact structure, and improved interfacial bonding between the fibers and matrix. These thermal results are supported by SEM data and are similar to those reported in previous studies [12,13].

### 3.4. Moisture absorption

Fig. 4 shows the effect of the vibration time on the percent moisture absorption of the biocomposite samples. The test was conducted for 8 h under conditions of RH = 75% and 25 °C. All biocomposite samples were saturated in less than 5 h. The percent moisture absorption of the VT 0 min biocomposite sample was 22%. This phenomenon was attributable to the nonhomogeneous dispersion of nanocellulose in the starch matrix. Another reason was the hydrophilic nature of starch and cellulose fibers [13].

These results differed from those of treated biocomposite samples, which exhibited less moisture absorption. For example, in the VT 60 min samples, the percent moisture absorption was 4.5% lower than that of the VT 0 min samples. This outcome occurred because the kinetic energy produced by the ultrasonic bath could reverse fiber agglomeration, homogeneously spread cellulose fibers in the starch matrix, and create a strong hydrogen bonding interaction between nanocellulose and the starch biopolymer. Accordingly, it was difficult for water molecules to diffuse into the matrix because of the formation of the tortuous path made by nanocellulose, the high moisture content of which created a barrier effect on the movement of water molecules through the biocomposite [12,13]. This result was supported by the FTIR characterization at a wavenumber of 1600  $\text{cm}^{-1}$ , which indicated water absorption by OH groups. Given the chemical similarity between nanocellulose and the starch biopolymers, the interfacial defects were reduced, thereby generating firm resistance to the flow of water molecules.

### 3.5. Functional group analysis

Fig. 5 shows the FTIR spectra of untreated and treated biocomposites. Three main peaks occurred at different wavenumbers (Fig. 5), namely 3000 (O–H stretching), 2900 (C–H stretching), and 1600  $\text{cm}^{-1}$  (water absorption by OH groups) [27,28].

O–H stretching appeared at 3000  $\text{cm}^{-1}$ , and the biocomposite displayed a shift to higher wavenumbers. This result

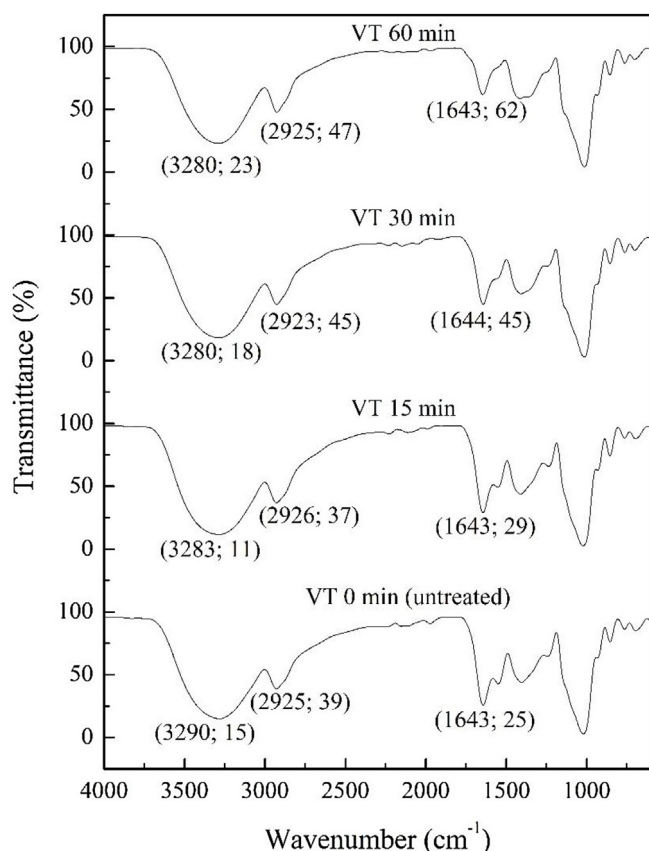


**Fig. 5 – Functional groups of all tested biocomposite samples. VT: vibration time.**

indicated an interaction between the matrix and fibers that generated new hydrogen bonds [28]. The transmittance values of the untreated and treated biocomposites varied. Long vibration times resulted in high transmittance values (Fig. 5) because of the greater OH stretching. Good hydrogen bonding was noted between the matrix and fibers (few occurrences of free OH) [12], thereby producing satisfactory tensile strength due to the good structure formation of OH molecules (crystalline) [6,12].

In addition, C–H stretching appeared at approximately  $2900\text{ cm}^{-1}$  in all biocomposite samples. Thus, all samples contained saturated aliphatic components, as reported by previous researchers [29]. Another phenomenon also appeared around  $1600\text{ cm}^{-1}$ . In this area, OH water absorption appears in each biocomposite sample. The transmittance value increases with the duration of vibration. The transmittance values of the VT 0, VT 15, VT 30, and VT 60 min biocomposite samples were 25%, 29%, 45%, and 62%, respectively. These results suggest that untreated biocomposite samples exhibit greater water absorption than treated samples [4,28]. This outcome was supported by the moisture absorption test results, in which the VT 0 min samples had the highest percent moisture absorption. However, treated biocomposite samples displayed lower moisture absorption. The kinetic energy of the ultrasonic bath could degrade the agglomerated nanocellulose fiber and spread them evenly in the matrix [12]. This phenomenon makes it difficult for water molecules to diffuse

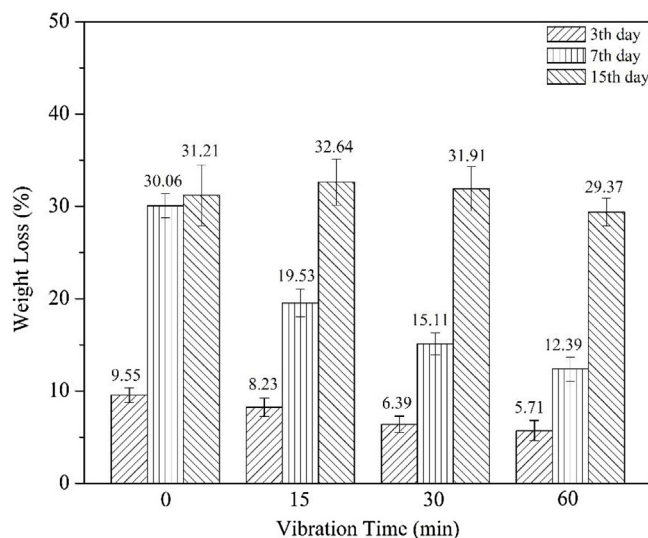


**Fig. 6 – Biodegradation rates of all tested biocomposite samples.**

into the matrix. A similar outcome was reported by previous research [6,12].

### 3.6. Soil biodegradation

Investigating soil biodegradation behavior is crucial for utilizing biocomposites in the environment. Soil biodegradation involves the degradation of materials by the action of microorganisms, fungi, bacteria, or other organisms that live in soil. Fig. 6 shows the effect of the vibration time on the biodegradation rates of all biocomposite samples. Compared with treated samples, untreated biocomposites exhibited greater weight loss. The percent weight loss on day 3 for untreated samples was 9.55%, and the values on days 7 and 15 were 30.06% and 31.21%, respectively. This outcome was supported by the results presented in Fig. 7a and b, in which the morphological structure depicts a large hole with an irregular configuration. This phenomenon may be attributable to fiber clumping in the matrix [8].

These values differed from those of VT 60 min samples. In these samples, the percent weight loss values were 5.71% (day 3), 12.39% (day 7), and 29.37% (day 15). Thus, VT 60 min samples had a slower degradation rate than the untreated samples. This phenomenon was attributable to the kinetic energy from the ultrasonic bath, which distributed the fibers homogeneously within the matrix [6]. The good fiber distribution in the matrix affected moisture, microorganisms, and other elements such that their diffusion into the matrix was difficult, as reported by previous research [14,15,30–32]. These results were supported by the SEM findings (Fig. 7c and d), in which the biocomposite structure was compact and less porous. The vibration time also decreased the biodegradation rate. These phenomena may be correlated with the water absorption properties of the biocomposite film, in which untreated film tends to absorb more water than treated film, thereby making the former more prone to attacks by microorganisms,

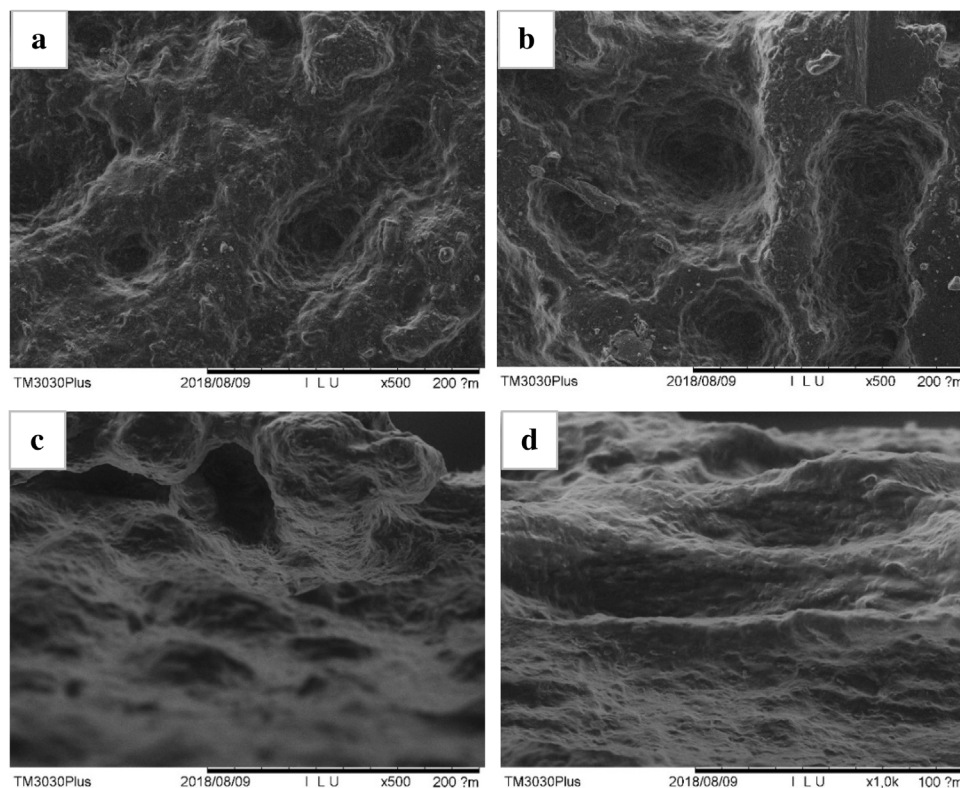


**Fig. 7 – Morphological characteristics of biocomposite samples after biodegradation in soil. (a) Untreated (day 3), (b) untreated (day 15), (c) vibrated for 60 min (day 3), and (d) vibrated for 60 min (day 15).**

which can attack the starch biopolymer in the presence of a water medium.

#### 4. Conclusion

Thermal stability and moisture resistance were successfully improved by vibration treatment using an ultrasonic bath instrument. Kinetic energy from the ultrasonic bath reduced the free OH bonding between the fiber and matrix. The best results were obtained for VT 60 min biocomposite samples. Increasing the vibration time also reduced the degradation rate of biocomposites in the soil. The soil burial test revealed that the vibrated biocomposites had slower biodegradation rates than the samples. The properties of the biocomposites suggest their potential application as environmentally friendly plastics for food packaging. The potential application of this biocomposite is food packaging, especially as packaging bags.

#### Conflicts of interest

The authors declare no conflict of interest regarding the publication of this manuscript. This manuscript has not been published and is not under consideration for publication elsewhere. The authors certify that neither the manuscript nor its main contents have been published or submitted for publication in another journal.

#### Acknowledgments

This work was financially supported by the Ministry of Research, Technology and Higher Education of the Republic of Indonesia (grant number 17/UN.16.17/PP.PMDSU/LPPM/2018). The authors thank Dr. Abukhalid Rivai, Dr. Ridwan and Dr. Gunawan of the Center for Science and Technology of Advanced Materials, National Nuclear Energy Agency, Indonesia for their support. Also, the authors would like to thank the UKM (GP-2019-K020448) for support.

#### REFERENCES

- [1] Li W, Tse HF, Fok L. Plastic waste in the marine environment: a review of sources, occurrence and effects. *Sci Total Environ* 2016;566:333–49, <http://dx.doi.org/10.1016/j.scitotenv.2016.05.084>.
- [2] Jambeck JR, Geyer R, Wilcox C, Siegler TR, Perryman M, Andrady A, et al. Plastic waste inputs from land into the ocean. *Science* 2015;347:768–71, <http://dx.doi.org/10.1126/science.1260352>.
- [3] Fahma F, Hori N, Iwata T, Takemura A. PVA nanocomposites reinforced with cellulose nanofibers from oil palm empty fruit bunches (OPEFBs). *Emir J Food Agric* 2017;29:323–9, <http://dx.doi.org/10.9755/ejfa.2016-02-215>.
- [4] Asrofi M, Abral H, Kasim A, Pratoto A, Mahardika M, Hafizulhaq F. Characterization of the sonicated yam bean starch bionanocomposites reinforced by nanocellulose water

- hyacinth fiber (WHF): the effect of various fiber loading. *J Eng Sci Technol* 2018;13:2700–15.
- [5] Gitari B, Chang BP, Misra M, Navabi A, Mohanty AK. A comparative study on the mechanical, thermal, and water barrier properties of PLA nanocomposite films prepared with bacterial nanocellulose and cellulose nanofibrils. *Bioresources* 2019;14:1867–89, <http://dx.doi.org/10.15376/biores.14.1.1867-1889>.
- [6] Asrofi M, Abrial H, Kasim A, Pratoto A, Mahardika M, Hafizulhaq F. Mechanical properties of a water hyacinth nanofiber cellulose reinforced thermoplastic starch bionanocomposite: effect of ultrasonic vibration during processing. *Fibers* 2018;6:40, <http://dx.doi.org/10.3390/fib6020040>.
- [7] Mali S, Grossmann MVE, Garcia MA, Martino MN, Zaritzky NE. Mechanical and thermal properties of yam starch films. *Food Hydrocoll* 2005;19:157–64, <http://dx.doi.org/10.1016/j.foodhyd.2004.05.002>.
- [8] Abrial H, Dalimunthe MH, Hartono J, Efendi RP, Asrofi M, Sugiarti E, et al. Characterization of tapioca starch biopolymer composites reinforced with micro scale water hyacinth fibers. *StarchStarke* 2018;70:1700287, <http://dx.doi.org/10.1002/star.201700287>.
- [9] Asrofi M, Abrial H, Kasim A, Pratoto A, Mahardika M, Park JW, et al. Isolation of nanocellulose from water hyacinth fiber (WHF) produced via digester-sonication and its characterization. *Fiber Polym* 2018;19:1618–25, <http://dx.doi.org/10.1007/s12221-018-7953-1>.
- [10] Dufresne A. Nanocellulose: a new ageless bionanomaterial. *Mater Today* 2013;16:220–7, <http://dx.doi.org/10.1016/j.mattod.2013.06.004>.
- [11] Ilyas RA, Sapuan SM, Ishak MR, Zainudin ES. Development and characterization of sugar palm nanocrystalline cellulose reinforced sugar palm starch bionanocomposites. *Carbohydr Polym* 2018;202:186–202, <http://dx.doi.org/10.1016/j.carbpol.2018.09.002>.
- [12] Abrial H, Putra GJ, Asrofi M, Park JW, Kim HJ. Effect of vibration duration of high ultrasound applied to bio-composite while gelatinized on its properties. *Ultrason Sonochem* 2018;40:697–702, <http://dx.doi.org/10.1016/j.ultrsonch.2017.08.019>.
- [13] Asrofi M, Abrial H, Putra YK, Sapuan SM, Kim HJ. Effect of duration of sonication during gelatinization on properties of tapioca starch water hyacinth fiber biocomposite. *Int J Biol Macromol* 2018;108:167–76, <http://dx.doi.org/10.1016/j.ijbiomac.2017.11.165>.
- [14] Phua YJ, Lau NS, Sudesh K, Chow WS, Ishak ZM. Biodegradability studies of poly (butylene succinate)/organo-montmorillonite nanocomposites under controlled compost soil conditions: effects of clay loading and compatibiliser. *Polym Degrad Stab* 2012;97:1345–54, <http://dx.doi.org/10.1016/j.polymdegradstab.2012.05.024>.
- [15] Bootklad M, Kaewtatip K. Biodegradation of thermoplastic starch/eggshell powder composites. *Carbohydr Polym* 2013;97:315–20, <http://dx.doi.org/10.1016/j.carbpol.2013.05.030>.
- [16] Mahardika M, Abrial H, Kasim A, Arief S, Asrofi M. Production of nanocellulose from pineapple leaf fibers via high-shear homogenization and ultrasonication. *Fibers* 2018;6:28, <http://dx.doi.org/10.3390/fib6020028>.
- [17] Ilyas RA, Sapuan SM, Ishak MR. Isolation and characterization of nanocrystalline cellulose from sugar palm fibres (*Arenga pinnata*). *Carbohydr Polym* 2018;181:1038–51, <http://dx.doi.org/10.1016/j.carbpol.2017.11.045>.
- [18] Asrofi M, Abrial H, Kasim A, Pratoto A. Characterization of the microfibrillated cellulose from water hyacinth pulp after alkali treatment and wet blending. *IOP Conf Ser Mater Sci Eng* 2017;204:012018, <http://dx.doi.org/10.1088/1757-899X/204/1/012018>.
- [19] Chen W, Yu H, Liu Y, Chen P, Zhang M, Hai Y. Individualization of cellulose nanofibers from wood using high-intensity ultrasonication combined with chemical pretreatments. *Carbohydr Polym* 2011;83:1804–11, <http://dx.doi.org/10.1016/j.carbpol.2010.10.040>.
- [20] Fahma F, Hori N, Iwamoto S, Iwata T, Takemura A. Cellulose nanowhiskers from sugar palm fibers. *Emir J Food Agric* 2016;28:566–71, <http://dx.doi.org/10.9755/efja.2016-02-188>.
- [21] Agustini MB, Ahmmad B, De Leon ERP, Buenaobra JL, Salazar JR, Hirose F. Starch-based biocomposite films reinforced with cellulose nanocrystals from garlic stalks. *Adv Manuf Polym Compos Sci* 2013;34:1325–32, <http://dx.doi.org/10.1002/pc.22546>.
- [22] Savadekar NR, Mhaske ST. Synthesis of nano cellulose fibers and effect on thermoplastics starch based films. *Carbohydr Polym* 2012;89:146–51, <http://dx.doi.org/10.1016/j.carbpol.2012.02.063>.
- [23] Syafri E, Kasim A, Abrial H, Sulungbudi GT, Sanjay MR, Sari NH. Synthesis and characterization of cellulose nanofibers (CNF) ramie reinforced cassava starch hybrid composites. *Int J Biol Macromol* 2018;120:578–86, <http://dx.doi.org/10.1016/j.ijbiomac.2018.08.134>.
- [24] Wahono S, Irwan A, Syafri E, Asrofi M. Preparation and characterization of ramie cellulose nanofibers/caco3 unsaturated polyester resin composites. *ARPN J Eng Appl Sci* 2018;13:746–51.
- [25] Lee SY, Mohan DJ, Kang IA, Doh GH, Lee S, Han SO. Nanocellulose reinforced PVA composite films: effects of acid treatment and filler loading. *Fiber Polym* 2009;10:77–82, <http://dx.doi.org/10.1007/s12221-009-0077-x>.
- [26] Martin AR, Martins MA, da Silva OR, Mattoso LH. Studies on the thermal properties of sisal fiber and its constituents. *Thermochim Acta* 2010;506:14–9, <http://dx.doi.org/10.1016/j.tca.2010.04.008>.
- [27] Asrofi M, Abrial H, Kasim A, Pratoto A. XRD and FTIR studies of nanocrystalline cellulose from water hyacinth (*Eichornia crassipes*) fiber. *J Metastable Nanocrystalline Mater* 2017;29:9–16, <http://dx.doi.org/10.4028/www.scientific.net/JMN.29.9>.
- [28] Kaewtatip K, Thongmee J. Studies on the structure and properties of thermoplastic starch/luffa fiber composites. *Mater Des* 2012;40:314–8, <http://dx.doi.org/10.1016/j.matdes.2012.03.053>.
- [29] Guleria A, Singha AS, Rana RK. Mechanical, thermal, morphological, and biodegradable studies of okra cellulosic fiber reinforced starch-based biocomposites. *Adv Polym Tech* 2016;37:104–12, <http://dx.doi.org/10.1002/adv.21646>.
- [30] Ilyas RA, Sapuan SM, Ishak MR, Zainudin ES. Sugar palm nanocrystalline cellulose reinforced sugar palm starch composite: degradation and water-barrier properties. *IOP Conf Series: Mater Sci Eng* 2018;368:012006, <http://dx.doi.org/10.1088/1757-899X/368/1/012006>.
- [31] Ilyas RA, Sapuan SM, Ishak MR, Zainudin ES. Sugar palm nanofibrillated cellulose (*Arenga pinnata* (Wurmb.) Merr): effect of cycles on their yield, physico-chemical, morphological and thermal behavior. *Int J Biol Macromol* 2019;123:379–88, <http://dx.doi.org/10.1016/j.ijbiomac.2018.11.124>.
- [32] Ilyas RA, Sapuan SM, Ibrahim R, Abrial H, Ishak MR, Zainudin ES, et al. Sugar palm (*Arenga pinnata* (Wurmb.) Merr) cellulosic fibre hierarchy: a comprehensive approach from macro to nano scale. *J Mater Res Technol* 2019, <http://dx.doi.org/10.1016/j.jmrt.2019.04.011>.

Available online at [www.sciencedirect.com](http://www.sciencedirect.com)

**jmr&t**  
Journal of Materials Research and Technology  
[www.jmrt.com.br](http://www.jmrt.com.br)



## Original Article

# Effect of sonication time on the thermal stability, moisture absorption, and biodegradation of water hyacinth (*Eichhornia crassipes*) nanocellulose-filled bengkuang (*Pachyrhizus erosus*) starch biocomposites



Edi Syafri<sup>a,\*</sup>, Sudirman<sup>b</sup>, Mashadi<sup>b</sup>, Evi Yulianti<sup>b</sup>, Deswita<sup>b</sup>, Mochamad Asrofi<sup>c</sup>, Hairul Abral<sup>d</sup>, S.M. Sapuan<sup>e,f</sup>, R.A. Ilyas<sup>e,f</sup>, Ahmad Fudholi<sup>g,\*</sup>

<sup>a</sup> Department of Agricultural Technology, Agricultural Polytechnic, Payakumbuh, West Sumatra 26271, Indonesia

<sup>b</sup> Center for Science and Technology of Advanced Materials, National Nuclear Energy Agency, Kawasan Nuklir, PUSPITEK Serpong, Banten, Indonesia

<sup>c</sup> Laboratory of Material Testing, Department of Mechanical Engineering, University of Jember, Kampus Tegalboto, Jember 68121, East Java, Indonesia

<sup>d</sup> Department of Mechanical Engineering, Andalas University, Kampus Limau Manis, Pauh, Padang 25163, Indonesia

<sup>e</sup> Laboratory of Biocomposite Technology, Institute of Tropical Forestry and Forest Products, Universiti Putra Malaysia, Serdang 43400, Selangor, Malaysia

<sup>f</sup> Department of Mechanical and Manufacturing Engineering, Universiti Putra Malaysia, Serdang 43400, Selangor, Malaysia

<sup>g</sup> Solar Energy Research Institute, Universiti Kebangsaan Malaysia, 43600 Bangi, Selangor, Malaysia

## ARTICLE INFO

## Article history:

Received 23 May 2019

Accepted 8 October 2019

Available online 13 November 2019

## Keywords:

Nanocellulose

Biodegradation

Biocomposites

Hyacinth fiber

Thermogravimetric analysis

## ABSTRACT

In Indonesia, starch, particularly that obtained from bengkuang (*Pachyrhizus erosus*), is abundant and inexpensive, thereby increasing the value of bengkuang starch, which can be mixed with bioplastic-based starch. A biocomposite comprising nanocellulose from water hyacinth (*Eichhornia crassipes*) and bengkuang starch was successfully fabricated using the solution casting method. Nanocellulose content in the matrix was kept constant at 1 wt%. Moreover, during fabrication, the biocomposite gel was treated in an ultrasonic bath for 0, 15, 30, and 60 min. Further, thermogravimetric analysis, moisture absorption measurements, Fourier transform infrared spectroscopy, and scanning electron microscopy were performed. The biocomposite sample vibrated for 60 min had the highest thermal stability and exhibited low moisture absorption. The soil burial test proved that this biocomposite, as opposed to 0-min vibrated samples, has a slower biodegradation rate. This result was supported by morphological evaluation after biodegradation, in which the 60-min vibrated samples showed a coarse surface and low porosity formation.

© 2019 The Authors. Published by Elsevier B.V. This is an open access article under the CC BY-NC-ND license (<http://creativecommons.org/licenses/by-nc-nd/4.0/>).

\* Corresponding author.

E-mails: [edi.syafri@politanipyk.ac.id](mailto:edi.syafri@politanipyk.ac.id) (E. Syafri), [a.fudholi@ukm.edu.my](mailto:a.fudholi@ukm.edu.my) (A. Fudholi).

<https://doi.org/10.1016/j.jmrt.2019.10.016>

2238-7854/© 2019 The Authors. Published by Elsevier B.V. This is an open access article under the CC BY-NC-ND license (<http://creativecommons.org/licenses/by-nc-nd/4.0/>).

## 1. Introduction

Plastic is widely used in many applications, including its use in food packaging, electronic components, and automotive dashboards. Usually, plastic is made using crude oil. However, plastic has a negative impact on the environment because it is nondegradable and it causes air pollution [1]. In 2010, Indonesia was responsible for the second highest level of marine plastic pollution after China. The total production of marine plastic debris globally ranges 0.48–1.29 million metric tons per year [2].

One breakthrough solution to this problem was the development of biodegradable plastic (bioplastic). Generally, bioplastic comprises starch, polylactic acid, and polyvinyl alcohol. In Indonesia, starch, especially that from bengkung (*Pachyrhizus erosus*), is abundant and inexpensive [3–5]. The total production of bengkung has reached 191.5 quintals/ha per year, thereby indirectly increasing the value of bengkung starch based on its ability to be mixed with bioplastic-based starch. Bengkulu starch has several advantages, namely its availability, low cost, and environmental friendliness. This starch has a high amylose content of approximately 30%–40% [6,7]. However, this starch has the disadvantages of low thermal stability and high moisture absorption [7]. The addition of cellulose fiber is an alternative solution to such problems.

Cellulose fiber from water hyacinth (*Eichhornia crassipes*) is a candidate for reinforcement because of its high cellulose content and abundance in nature [8,9]. Water hyacinth is a free-floating macrophyte that exhibits a fast growth rate, adaptability to a wide range of environmental conditions, and high nutrient uptake capacity. Cellulose in the nanometer range, called nanocellulose, has become prevalent in recent years. Nanocellulose has several advantages, such as being biodegradable and renewable and having acceptable transparency [10,11]. Prior research established that the addition of nanocellulose in the matrix increased thermal and moisture resistance.

However, these properties depend on several factors, including porosity, the agglomeration phenomenon, and the dispersion of nanocellulose in the matrix [12]. Ultrasonication is used to reduce the formation of agglomeration and increase the dispersity of nanocellulose in fibers. Several studies reported the use of ultrasonic treatment of nanocellulose for reducing agglomeration during gelatinization. Previous researchers prepared and sonicated biocomposites from cellulose fiber-reinforced starch during gelatinization using an ultrasonic bath instrument. They claimed that sonication successfully reduced fiber agglomeration in the starch matrix [12,13]. However, their work did not reveal the biodegradation characteristic of the biocomposite sample. Note that biodegradation has an important role in biocomposites, as previously reported [14,15].

Several researchers have investigated the use of distilled water to clean samples after biodegradation in soil [14,15]. However, this method is ineffective for separating soil from samples. Soil continues to adhere to samples because of the lowest-energy water, as substantiated by several experiments. Accordingly, this work proposed a new method for

cleaning samples. Using an ultrasonic bath is an effective means of separating soil from samples after biodegradation. The morphological characteristics of samples after biodegradation were observed via scanning electron microscopy (SEM). Thermogravimetric analysis (TGA), moisture absorption measurements, and Fourier transform infrared (FTIR) spectrometry were conducted to determine thermal stability, moisture resistance, and the functional group of the biocomposites, respectively. This study aimed to investigate the effect of the vibration (sonication) duration (0, 15, 30, or 60 min) during the fabrication of biocomposite samples, specifically focusing on thermal stability, moisture resistance, and biodegradation in soil.

## 2. Materials and methods

### 2.1. Materials

Water hyacinth fiber was obtained from Payakumbuh, Indonesia. Nanocellulose was obtained from water hyacinth fiber via chemical and mechanical treatment. The lignin, hemicellulose, and cellulose contents of water hyacinth were 7%, 29%, and 43%, respectively. Bengkulu tubers were purchased from local farmers in Kuranji, Padang, Indonesia. All chemical reagents, such as distilled water, glycerol, NaOH, NaClO<sub>2</sub>, CH<sub>3</sub>COOH, and HCl, were obtained from the Metallurgy Mechanic Laboratory, Andalas University.

### 2.2. Extraction of bengkung starch

Bengkung tubers were peeled, cut into small pieces, and then crushed using an ice blender at 10,000 rpm for 5 min to obtain the resulting porridge. The porridge was filtered using a mesh screen (200 mesh) to separate the bagasse and suspension. Furthermore, the suspension was precipitated for 5 h to acquire the bengkung starch. The precipitant was dried in an oven at 50 °C for 20 h. Then, the resulting material was collected and crushed to produce dry starch powder.

### 2.3. Isolation of nanocellulose from water hyacinth

Water hyacinth fiber was prepared as previously described [9]. Dried water hyacinth fiber (15 g) was pulped using 15% sodium hydroxide solution. The mixture was heated and stirred at 60 °C and 300 rpm for 4 h. Then, the fiber was cleaned from the alkali solution with distilled water. Bleaching was performed using sodium chlorite and acetic acid (4:1). This process was conducted at 60 °C and 300 rpm for 2 h. The mixture was rinsed with distilled water to obtain the cellulose suspension. Next, 5 M HCl was added to the suspension for acid hydrolysis at 60 °C and 300 rpm for 20 h. HCl was used to isolate nanocellulose from the cellulose fiber. Then, the products were neutralized using distilled water before ultrasonication. An ultrasonic crusher was utilized to produce nanocellulose from water hyacinth. This process was conducted at 600 W for 1 h.

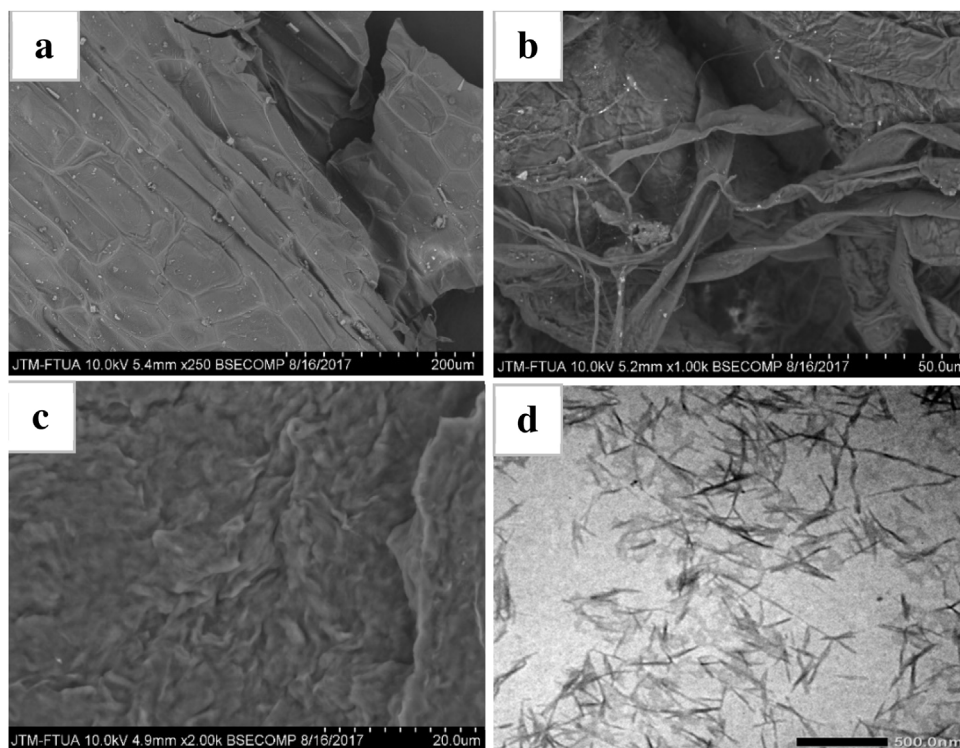


**Fig. 1 – Water hyacinth fiber before and after treatment. (a) Raw fiber (untreated), (b) bleached fiber, (c) fiber subjected to acid hydrolysis; and (d) fiber subjected to ultrasonication.**

#### 2.4. Biocomposite fabrication

A total of 10 g of bengkuang starch was mixed with 100 ml of distilled water in a glass beaker. This mixture was homogenized using an ultrasonic homogenizer at 8000 rpm for 5 min. During homogenization, 1% NWHF and 2 ml of glycerol were slowly added to the mixing solution. A constant fraction of nanocellulose (1 wt%) was used as reinforcement in the bengkuang starch matrix. Then, the mixing solution was heated and stirred at 60 °C and 500 rpm for 30 min (until gelatinized). The biocomposite gel (70 g) was poured in a Petri dish (15 cm diameter). The gel was incubated in an ultrasonic bath for 0, 15, 30, or 60 min and labeled as VT 0 (untreated), VT 15, VT 30, and VT 60, respectively. Subsequently, the biocomposite was dried in a drying oven at 50 °C for 20 h.

#### 2.5. Characterization

##### 2.5.1. SEM

The morphology of the untreated and treated water hyacinth fibers as well as the morphological characteristic of all biocomposites tested after biodegradation in soil were observed using a Hitachi 3400 N scanning electron microscope. The operation voltage was 10 kV. The fracture surface of the biocomposite was studied through a VEGA3 TESCAN SEM instrument at room temperature and 10 kV. All samples were coated with gold using an argon plasma metalizer (sputter coater K575X, Edwards Limited, Crawley, UK) to avoid charging.

##### 2.5.2. Transmission electron microscopy (TEM)

A JEM-JEOL 1400 TEM instrument was operated at 100 keV to observe the nanocellulose fibers. The nanocellulose suspension was cast in a carbon-coated grid and then directly observed at room temperature.

##### 2.5.3. Thermogravimetric analysis

All samples were tested using a TGA/DTG 60 system (serial no. C30565000570) to determine the thermal degradation point at each stage. The test was conducted over the temperature range of 30 °C–550 °C under a nitrogen atmosphere. The heating rate was maintained at 10 °C/min. The weight of all tested samples was 5–7 mg.

##### 2.5.4. Moisture absorption

All tested samples were cut into 1 cm × 3 cm pieces and dried in a drying oven to a constant weight. The initial ( $W_0$ ) and final weights ( $W_t$ ) were recorded. Moisture absorption was examined in a moisture chamber (relative humidity [RH]: 75%) at 25 °C. The percent moisture absorption was calculated using the following equation [12]:

$$\text{Moisture Absorption} = \frac{W_t - W_0}{W_0} \times 100\%. \quad (1)$$

##### 2.5.5. FTIR spectroscopy

FTIR spectroscopy was used to determine the functional groups of all samples. The FTIR spectrum of all tested samples was recorded using a Perkin-Elmer Frontier FTIR instrument

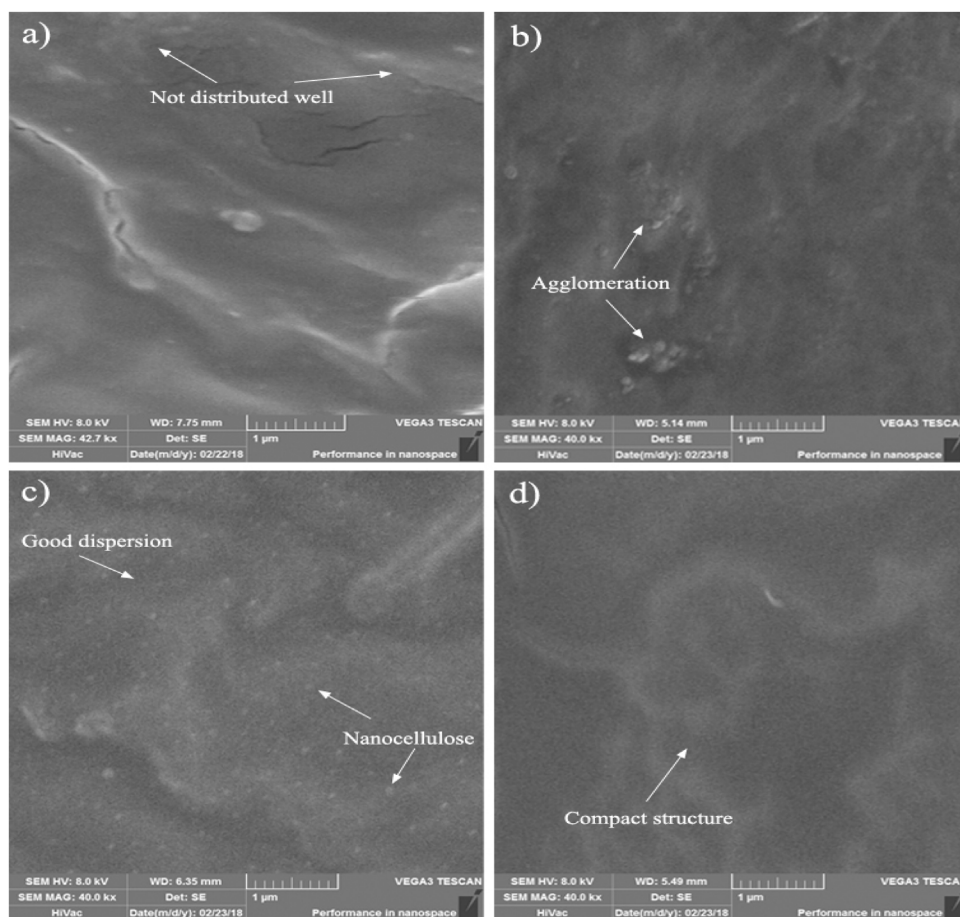


**Fig. 2 – Fracture surface of all biocomposite samples. Samples were vibrated for (a) 0, (b) 15, (c) 30, or (d) 60 min.**

with a resolution of  $4\text{ cm}^{-1}$ . The scanned wavenumber range was  $600\text{--}4000\text{ cm}^{-1}$ .

### 2.5.6. Soil burial test

The biodegradation test was conducted by burying the samples in soil that was purchased from PT. Mahesa Mutiara Tani (Kompos Nesia, Bogor, Indonesia). The soil contained organic carbon (34.25%), nitrogen (2%), ferrous (7.9%), pH (7.33), diphosphorus pentoxide (0.62%), other materials (e.g., plastic, glass, gravel = 0.1%), and several colonies in 1 g of soil ( $8 \times 10^{14}$  CFU), and its carbon-to-nitrogen ratio was 17.15%.

**Control sample:** The sample was cut into  $10\text{ mm} \times 10\text{ mm}$  pieces and then dried in a drying oven at  $50^\circ\text{C}$  for 20 h to a constant weight. Then, the sample was subjected to ultrasonic bath treatment for 5 min and dried in an oven at  $50^\circ\text{C}$  for 20 h. Subsequently, the sample was weighed using a precision balance (accuracy = 0.001). The weight loss of the control sample was calculated as the difference between  $W_0$  before ultrasonic bath treatment and  $W_t$  after the treatment.

**Buried samples:** All samples for the burial test measured  $10\text{ mm} \times 10\text{ mm}$ . The samples were dried in a drying oven at  $50^\circ\text{C}$  for 20 h to a constant weight and weighed using a precision balance to obtain  $W_0$  before burial in soil. Then, the test was conducted in a square container ( $10\text{ cm} \times 10\text{ cm}$ ) containing soil an RH and temperature of 60%–65% and  $25^\circ\text{C}$ ,

respectively. After vibration, biodegradation was observed after 3, 7, and 15 days of burial in soil.

After burial, all samples were collected and cleaned using a paintbrush. Then, the samples were subjected to ultrasonic bath treatment for 5 min to remove the soil that adhered to the biocomposites. The samples were dried in a drying oven at  $50^\circ\text{C}$  for 20 h to a constant weight. Afterward, they were weighed using an analytical balance. The percent weight loss of the sample due to soil burial was calculated according to the different weights before and after the burial test. The percent weight loss due to soil was calculated using the following equation:

$$W_{\text{degradation}} = W_{\text{burial test}} - W_{\text{control}} \quad (2)$$

## 3. Results and discussion

### 3.1. Morphological characteristics of untreated and treated fibers

Fig. 1 shows the morphological features of water hyacinth fiber before and after treatment. Fig. 1a displays the raw water hyacinth fiber (untreated), which had a smooth surface, and some microfibrils were still bound. Untreated fiber contains lignin substances such as waxes and oils [16,17]. Bleaching

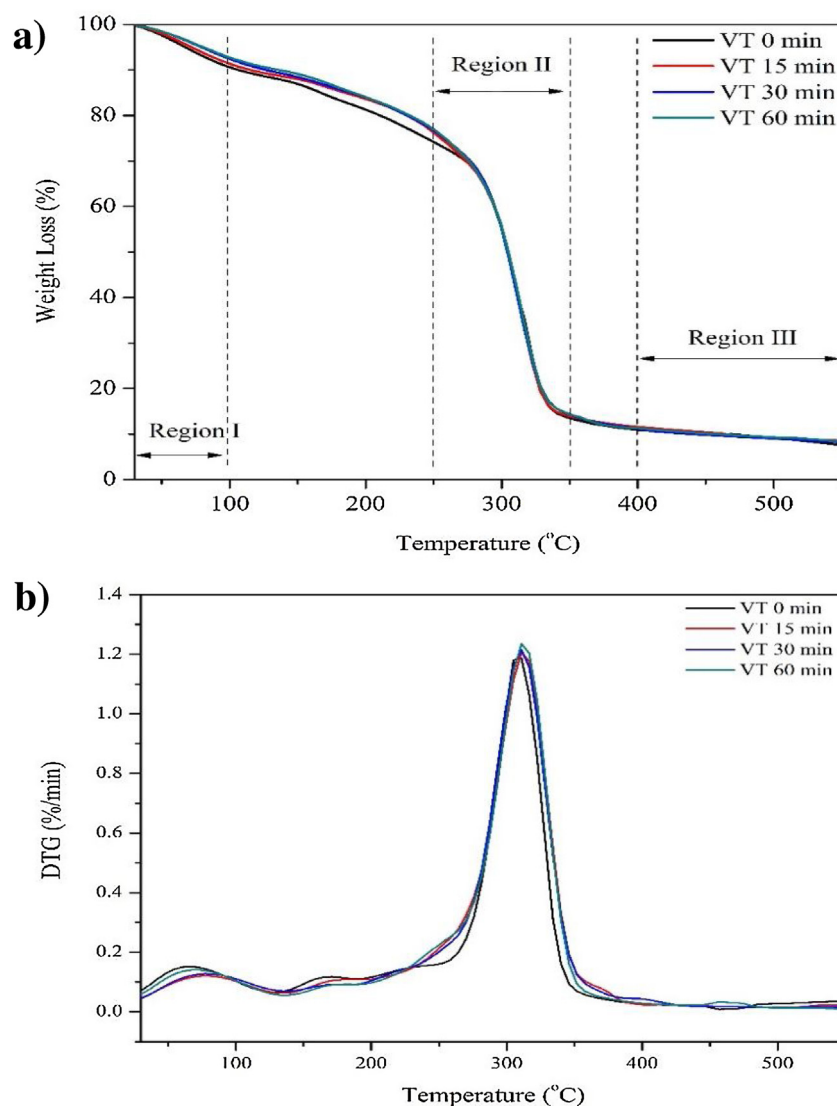


**Fig. 3 – (a) Thermogravimetric analysis and (b) DTG curves of all biocomposite samples.**

successfully destroyed several microfibril bonds, as presented in Fig. 1b, because of the broken linkage between lignin and hemicellulose. A similar phenomenon was reported by a previous study [9,18]. In the acid hydrolysis process (Fig. 1c), the fiber was depolymerized into short individual microfibrils with a diameter and length of 2 and 6 microns, respectively. Nanocellulose was obtained via ultrasonication for 1 h. Fig. 1d displays the distribution of cellulose fibers in the nanometer range. Cellulose fibers were dispersed homogeneously, as shown in the TEM images (Fig. 1d), measuring 15 nm in diameter and 147 nm in length. This outcome is attributable to the high intensity of the power ultrasound, resulting in short cellulose fibers in the nanometer range [19,20].

### 3.2. Fracture surface of the biocomposites

Fig. 2 shows the fracture surface of untreated and treated biocomposite films. Fig. 2a displays the fracture morphology of the VT 0 min sample (untreated). The cellulose fibers in bengkuan starch were not distributed well. Thus, the mixing

of starch and cellulose was not homogeneous during fabrication [21]. This explained the low thermal stability of the untreated biocomposite. A poor distribution of nanocellulose affects thermal stability in terms of interfacial adhesion between the nanocellulose and starch biopolymers. That is, the strong interfacial adhesion between nanocellulose and starch corresponded to the high thermal stability of the biocomposites because a high temperature is required to break the bonds between nanocellulose and starch biopolymers.

The VT 15 min sample also exhibited no significant fracture morphology. The agglomeration phenomenon remains apparent in this sample (Fig. 2b). According to a previous report, agglomeration and poor dispersion of cellulose fibers lead to decreased thermal and moisture resistance [22]. The different fracture morphologies are shown in Fig. 2c and d for the VT 30 min and VT 60 min samples, respectively. In these cases, the samples displayed good dispersion and compact structures. These findings are probably attributable to the kinetic energy from the ultrasonic bath, leading to improved interfacial bonding between the fibers and matrix [12,13]. This

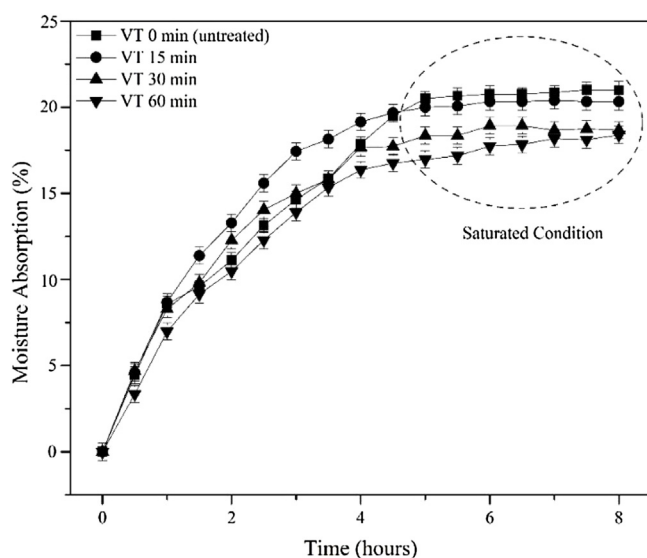


**Fig. 4 – Moisture absorption of all tested biocomposite samples. Samples were subjected to ultrasonication for 0, 15, 30, or 60 min. VT: vibration time.**

treatment also resulted in good dispersion of the nanocellulose in the matrix and reduced the free OH bonding between the fibers and matrix. This phenomenon was similar to that observed by Asrofi et al. [6] concerning the effect of ultrasonic vibration during processing on the mechanical properties of a water hyacinth nanofiber cellulose-reinforced thermoplastic starch bionanocomposite.

### 3.3. Thermal stability

The thermal characteristics of the biocomposite samples with various vibration times were presented using TGA (Fig. 3a) and DTG (Fig. 3b) curves. Two main degradation areas were found in accordance with the results from previous research [23–25]. The first region of degradation reflected the initial degradation of all biocomposite samples at temperatures of less than 100 °C as indicated by the TGA and DTG curves. This result revealed increasing weight loss compared with  $W_0$  before testing. The percent weight loss values of the biocomposite in the first region were 11% (VT 0 min), 9% (VT 15 min), 9% (VT 30 min), and 7% (VT 60 min). This phenomenon was attributable to the moisture content in all samples [8,25]. These results were supported by the DTG curve (Fig. 1b), which reveals the presence of small peaks in the temperature range of 50 °C–100 °C.

The second region (250 °C–350 °C) involved significant weight loss exceeding 50% for all samples. In this condition, the structures of starch, glycerol, and nanocellulose fibers were degraded [12,26]. The DTG curve (Fig. 1b) exhibits a sharp peak due to the significant weight reduction. The degradation temperatures for all samples in this area was 305 °C, 309 °C, 311 °C, and 318 °C for VT 0, VT 15, VT 30, and VT 60 min, respectively. Untreated biocomposite samples (VT 0) min had lower degradation temperatures. This outcome indicated fiber agglomerated and porosity formation in the matrix that resulted in reduced thermal stability [4]. Thermal stability

and moisture resistance increased with prolonged ultrasonic vibration.

Conversely, increased vibration time improved the thermal stability of the biocomposite samples. This result was supported by the increase in the degradation temperature of the treated samples compared with that of the untreated sample due to the improved interfacial adhesion between the fibers and matrix as a result of the kinetic energy of the ultrasonic bath. Good adhesion was indicated by the scarcity of free OH between the fibers and matrix [6,8,12].

In the third region (>400 °C), all samples were completely decomposed, becoming ash [25,26]. However, the treated samples had higher thermal stability than untreated samples because of the kinetic energy of the ultrasonic bath, which allowed the fibers to disperse evenly in the matrix. Other effects of the bath included good dispersion of the fibers in the matrix, a compact structure, and improved interfacial bonding between the fibers and matrix. These thermal results are supported by SEM data and are similar to those reported in previous studies [12,13].

### 3.4. Moisture absorption

Fig. 4 shows the effect of the vibration time on the percent moisture absorption of the biocomposite samples. The test was conducted for 8 h under conditions of RH = 75% and 25 °C. All biocomposite samples were saturated in less than 5 h. The percent moisture absorption of the VT 0 min biocomposite sample was 22%. This phenomenon was attributable to the nonhomogeneous dispersion of nanocellulose in the starch matrix. Another reason was the hydrophilic nature of starch and cellulose fibers [13].

These results differed from those of treated biocomposite samples, which exhibited less moisture absorption. For example, in the VT 60 min samples, the percent moisture absorption was 4.5% lower than that of the VT 0 min samples. This outcome occurred because the kinetic energy produced by the ultrasonic bath could reverse fiber agglomeration, homogeneously spread cellulose fibers in the starch matrix, and create a strong hydrogen bonding interaction between nanocellulose and the starch biopolymer. Accordingly, it was difficult for water molecules to diffuse into the matrix because of the formation of the tortuous path made by nanocellulose, the high moisture content of which created a barrier effect on the movement of water molecules through the biocomposite [12,13]. This result was supported by the FTIR characterization at a wavenumber of 1600  $\text{cm}^{-1}$ , which indicated water absorption by OH groups. Given the chemical similarity between nanocellulose and the starch biopolymers, the interfacial defects were reduced, thereby generating firm resistance to the flow of water molecules.

### 3.5. Functional group analysis

Fig. 5 shows the FTIR spectra of untreated and treated biocomposites. Three main peaks occurred at different wavenumbers (Fig. 5), namely 3000 (O–H stretching), 2900 (C–H stretching), and 1600  $\text{cm}^{-1}$  (water absorption by OH groups) [27,28].

O–H stretching appeared at 3000  $\text{cm}^{-1}$ , and the biocomposite displayed a shift to higher wavenumbers. This result

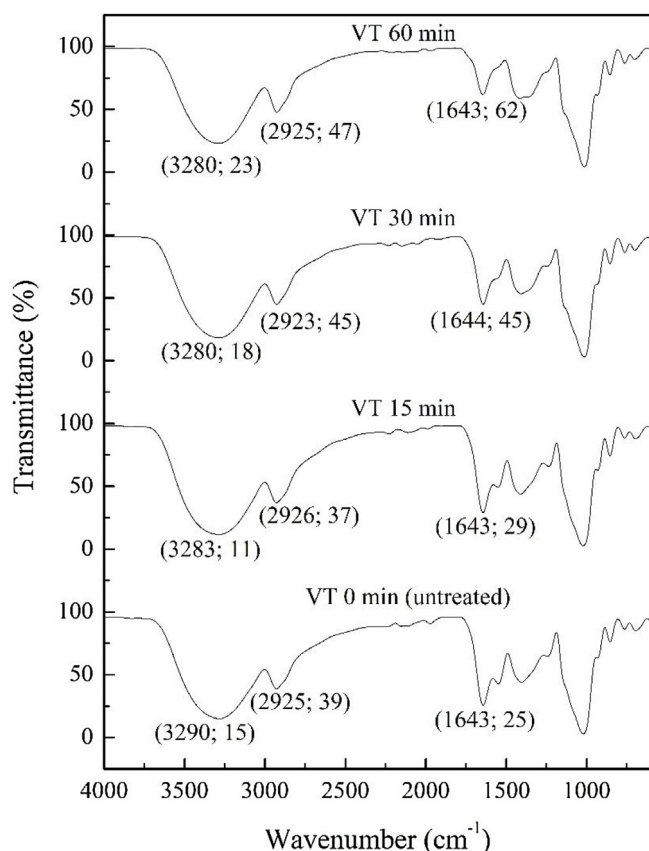


**Fig. 5 – Functional groups of all tested biocomposite samples. VT: vibration time.**

indicated an interaction between the matrix and fibers that generated new hydrogen bonds [28]. The transmittance values of the untreated and treated biocomposites varied. Long vibration times resulted in high transmittance values (Fig. 5) because of the greater OH stretching. Good hydrogen bonding was noted between the matrix and fibers (few occurrences of free OH) [12], thereby producing satisfactory tensile strength due to the good structure formation of OH molecules (crystalline) [6,12].

In addition, C–H stretching appeared at approximately  $2900\text{ cm}^{-1}$  in all biocomposite samples. Thus, all samples contained saturated aliphatic components, as reported by previous researchers [29]. Another phenomenon also appeared around  $1600\text{ cm}^{-1}$ . In this area, OH water absorption appears in each biocomposite sample. The transmittance value increases with the duration of vibration. The transmittance values of the VT 0, VT 15, VT 30, and VT 60 min biocomposite samples were 25%, 29%, 45%, and 62%, respectively. These results suggest that untreated biocomposite samples exhibit greater water absorption than treated samples [4,28]. This outcome was supported by the moisture absorption test results, in which the VT 0 min samples had the highest percent moisture absorption. However, treated biocomposite samples displayed lower moisture absorption. The kinetic energy of the ultrasonic bath could degrade the agglomerated nanocellulose fiber and spread them evenly in the matrix [12]. This phenomenon makes it difficult for water molecules to diffuse

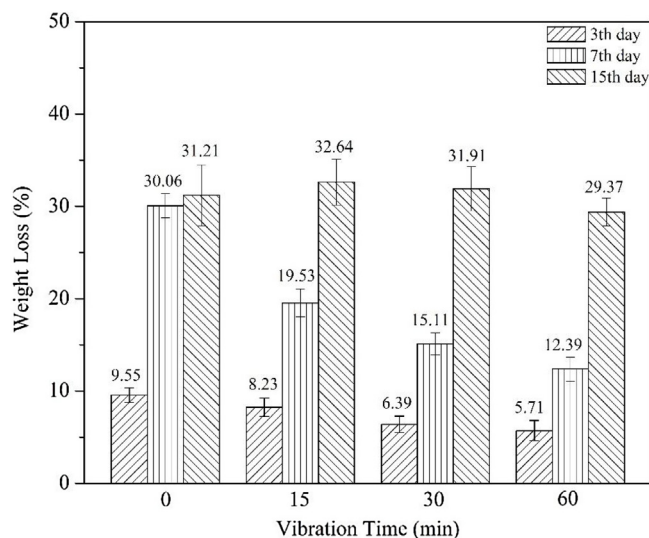


**Fig. 6 – Biodegradation rates of all tested biocomposite samples.**

into the matrix. A similar outcome was reported by previous research [6,12].

### 3.6. Soil biodegradation

Investigating soil biodegradation behavior is crucial for utilizing biocomposites in the environment. Soil biodegradation involves the degradation of materials by the action of microorganisms, fungi, bacteria, or other organisms that live in soil. Fig. 6 shows the effect of the vibration time on the biodegradation rates of all biocomposite samples. Compared with treated samples, untreated biocomposites exhibited greater weight loss. The percent weight loss on day 3 for untreated samples was 9.55%, and the values on days 7 and 15 were 30.06% and 31.21%, respectively. This outcome was supported by the results presented in Fig. 7a and b, in which the morphological structure depicts a large hole with an irregular configuration. This phenomenon may be attributable to fiber clumping in the matrix [8].

These values differed from those of VT 60 min samples. In these samples, the percent weight loss values were 5.71% (day 3), 12.39% (day 7), and 29.37% (day 15). Thus, VT 60 min samples had a slower degradation rate than the untreated samples. This phenomenon was attributable to the kinetic energy from the ultrasonic bath, which distributed the fibers homogeneously within the matrix [6]. The good fiber distribution in the matrix affected moisture, microorganisms, and other elements such that their diffusion into the matrix was difficult, as reported by previous research [14,15,30–32]. These results were supported by the SEM findings (Fig. 7c and d), in which the biocomposite structure was compact and less porous. The vibration time also decreased the biodegradation rate. These phenomena may be correlated with the water absorption properties of the biocomposite film, in which untreated film tends to absorb more water than treated film, thereby making the former more prone to attacks by microorganisms,

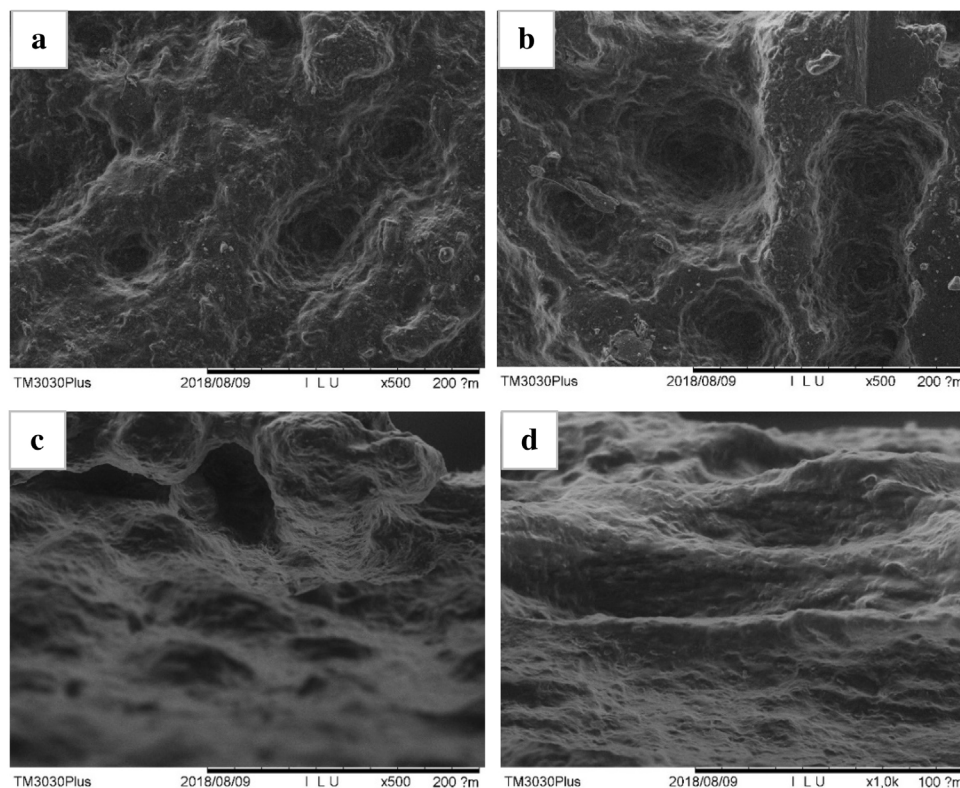


**Fig. 7 – Morphological characteristics of biocomposite samples after biodegradation in soil. (a) Untreated (day 3), (b) untreated (day 15), (c) vibrated for 60 min (day 3), and (d) vibrated for 60 min (day 15).**

which can attack the starch biopolymer in the presence of a water medium.

#### 4. Conclusion

Thermal stability and moisture resistance were successfully improved by vibration treatment using an ultrasonic bath instrument. Kinetic energy from the ultrasonic bath reduced the free OH bonding between the fiber and matrix. The best results were obtained for VT 60 min biocomposite samples. Increasing the vibration time also reduced the degradation rate of biocomposites in the soil. The soil burial test revealed that the vibrated biocomposites had slower biodegradation rates than the samples. The properties of the biocomposites suggest their potential application as environmentally friendly plastics for food packaging. The potential application of this biocomposite is food packaging, especially as packaging bags.

#### Conflicts of interest

The authors declare no conflict of interest regarding the publication of this manuscript. This manuscript has not been published and is not under consideration for publication elsewhere. The authors certify that neither the manuscript nor its main contents have been published or submitted for publication in another journal.

#### Acknowledgments

This work was financially supported by the Ministry of Research, Technology and Higher Education of the Republic of Indonesia (grant number 17/UN.16.17/PP.PMDSU/LPPM/2018). The authors thank Dr. Abukhalid Rivai, Dr. Ridwan and Dr. Gunawan of the Center for Science and Technology of Advanced Materials, National Nuclear Energy Agency, Indonesia for their support. Also, the authors would like to thank the UKM (GP-2019-K020448) for support.

#### REFERENCES

- [1] Li W, Tse HF, Fok L. Plastic waste in the marine environment: a review of sources, occurrence and effects. *Sci Total Environ* 2016;566:333–49, <http://dx.doi.org/10.1016/j.scitotenv.2016.05.084>.
- [2] Jambeck JR, Geyer R, Wilcox C, Siegler TR, Perryman M, Andrady A, et al. Plastic waste inputs from land into the ocean. *Science* 2015;347:768–71, <http://dx.doi.org/10.1126/science.1260352>.
- [3] Fahma F, Hori N, Iwata T, Takemura A. PVA nanocomposites reinforced with cellulose nanofibers from oil palm empty fruit bunches (OPEFBs). *Emir J Food Agric* 2017;29:323–9, <http://dx.doi.org/10.9755/ejfa.2016-02-215>.
- [4] Asrofi M, Abral H, Kasim A, Pratoto A, Mahardika M, Hafizulhaq F. Characterization of the sonicated yam bean starch bionanocomposites reinforced by nanocellulose water

- hyacinth fiber (WHF): the effect of various fiber loading. *J Eng Sci Technol* 2018;13:2700–15.
- [5] Gitari B, Chang BP, Misra M, Navabi A, Mohanty AK. A comparative study on the mechanical, thermal, and water barrier properties of PLA nanocomposite films prepared with bacterial nanocellulose and cellulose nanofibrils. *Bioresources* 2019;14:1867–89, <http://dx.doi.org/10.15376/biores.14.1.1867-1889>.
- [6] Asrofi M, Abrial H, Kasim A, Pratoto A, Mahardika M, Hafizulhaq F. Mechanical properties of a water hyacinth nanofiber cellulose reinforced thermoplastic starch bionanocomposite: effect of ultrasonic vibration during processing. *Fibers* 2018;6:40, <http://dx.doi.org/10.3390/fib6020040>.
- [7] Mali S, Grossmann MVE, Garcia MA, Martino MN, Zaritzky NE. Mechanical and thermal properties of yam starch films. *Food Hydrocoll* 2005;19:157–64, <http://dx.doi.org/10.1016/j.foodhyd.2004.05.002>.
- [8] Abrial H, Dalimunthe MH, Hartono J, Efendi RP, Asrofi M, Sugiarti E, et al. Characterization of tapioca starch biopolymer composites reinforced with micro scale water hyacinth fibers. *StarchStarke* 2018;70:1700287, <http://dx.doi.org/10.1002/star.201700287>.
- [9] Asrofi M, Abrial H, Kasim A, Pratoto A, Mahardika M, Park JW, et al. Isolation of nanocellulose from water hyacinth fiber (WHF) produced via digester-sonication and its characterization. *Fiber Polym* 2018;19:1618–25, <http://dx.doi.org/10.1007/s12221-018-7953-1>.
- [10] Dufresne A. Nanocellulose: a new ageless bionanomaterial. *Mater Today* 2013;16:220–7, <http://dx.doi.org/10.1016/j.mattod.2013.06.004>.
- [11] Ilyas RA, Sapuan SM, Ishak MR, Zainudin ES. Development and characterization of sugar palm nanocrystalline cellulose reinforced sugar palm starch bionanocomposites. *Carbohydr Polym* 2018;202:186–202, <http://dx.doi.org/10.1016/j.carbpol.2018.09.002>.
- [12] Abrial H, Putra GJ, Asrofi M, Park JW, Kim HJ. Effect of vibration duration of high ultrasound applied to bio-composite while gelatinized on its properties. *Ultrason Sonochem* 2018;40:697–702, <http://dx.doi.org/10.1016/j.ultrsonch.2017.08.019>.
- [13] Asrofi M, Abrial H, Putra YK, Sapuan SM, Kim HJ. Effect of duration of sonication during gelatinization on properties of tapioca starch water hyacinth fiber biocomposite. *Int J Biol Macromol* 2018;108:167–76, <http://dx.doi.org/10.1016/j.ijbiomac.2017.11.165>.
- [14] Phua YJ, Lau NS, Sudesh K, Chow WS, Ishak ZM. Biodegradability studies of poly (butylene succinate)/organo-montmorillonite nanocomposites under controlled compost soil conditions: effects of clay loading and compatibiliser. *Polym Degrad Stab* 2012;97:1345–54, <http://dx.doi.org/10.1016/j.polymdegradstab.2012.05.024>.
- [15] Bootklad M, Kaewtatip K. Biodegradation of thermoplastic starch/eggshell powder composites. *Carbohydr Polym* 2013;97:315–20, <http://dx.doi.org/10.1016/j.carbpol.2013.05.030>.
- [16] Mahardika M, Abrial H, Kasim A, Arief S, Asrofi M. Production of nanocellulose from pineapple leaf fibers via high-shear homogenization and ultrasonication. *Fibers* 2018;6:28, <http://dx.doi.org/10.3390/fib6020028>.
- [17] Ilyas RA, Sapuan SM, Ishak MR. Isolation and characterization of nanocrystalline cellulose from sugar palm fibres (*Arenga pinnata*). *Carbohydr Polym* 2018;181:1038–51, <http://dx.doi.org/10.1016/j.carbpol.2017.11.045>.
- [18] Asrofi M, Abrial H, Kasim A, Pratoto A. Characterization of the microfibrillated cellulose from water hyacinth pulp after alkali treatment and wet blending. *IOP Conf Ser Mater Sci Eng* 2017;204:012018, <http://dx.doi.org/10.1088/1757-899X/204/1/012018>.
- [19] Chen W, Yu H, Liu Y, Chen P, Zhang M, Hai Y. Individualization of cellulose nanofibers from wood using high-intensity ultrasonication combined with chemical pretreatments. *Carbohydr Polym* 2011;83:1804–11, <http://dx.doi.org/10.1016/j.carbpol.2010.10.040>.
- [20] Fahma F, Hori N, Iwamoto S, Iwata T, Takemura A. Cellulose nanowhiskers from sugar palm fibers. *Emir J Food Agric* 2016;28:566–71, <http://dx.doi.org/10.9755/efja.2016-02-188>.
- [21] Agustini MB, Ahmmad B, De Leon ERP, Buenaobra JL, Salazar JR, Hirose F. Starch-based biocomposite films reinforced with cellulose nanocrystals from garlic stalks. *Adv Manuf Polym Compos Sci* 2013;34:1325–32, <http://dx.doi.org/10.1002/pc.22546>.
- [22] Savadekar NR, Mhaske ST. Synthesis of nano cellulose fibers and effect on thermoplastics starch based films. *Carbohydr Polym* 2012;89:146–51, <http://dx.doi.org/10.1016/j.carbpol.2012.02.063>.
- [23] Syafri E, Kasim A, Abrial H, Sulungbudi GT, Sanjay MR, Sari NH. Synthesis and characterization of cellulose nanofibers (CNF) ramie reinforced cassava starch hybrid composites. *Int J Biol Macromol* 2018;120:578–86, <http://dx.doi.org/10.1016/j.ijbiomac.2018.08.134>.
- [24] Wahono S, Irwan A, Syafri E, Asrofi M. Preparation and characterization of ramie cellulose nanofibers/caco3 unsaturated polyester resin composites. *ARPN J Eng Appl Sci* 2018;13:746–51.
- [25] Lee SY, Mohan DJ, Kang IA, Doh GH, Lee S, Han SO. Nanocellulose reinforced PVA composite films: effects of acid treatment and filler loading. *Fiber Polym* 2009;10:77–82, <http://dx.doi.org/10.1007/s12221-009-0077-x>.
- [26] Martin AR, Martins MA, da Silva OR, Mattoso LH. Studies on the thermal properties of sisal fiber and its constituents. *Thermochim Acta* 2010;506:14–9, <http://dx.doi.org/10.1016/j.tca.2010.04.008>.
- [27] Asrofi M, Abrial H, Kasim A, Pratoto A. XRD and FTIR studies of nanocrystalline cellulose from water hyacinth (*Eichornia crassipes*) fiber. *J Metastable Nanocrystalline Mater* 2017;29:9–16, <http://dx.doi.org/10.4028/www.scientific.net/JMN.29.9>.
- [28] Kaewtatip K, Thongmee J. Studies on the structure and properties of thermoplastic starch/luffa fiber composites. *Mater Des* 2012;40:314–8, <http://dx.doi.org/10.1016/j.matdes.2012.03.053>.
- [29] Guleria A, Singha AS, Rana RK. Mechanical, thermal, morphological, and biodegradable studies of okra cellulosic fiber reinforced starch-based biocomposites. *Adv Polym Tech* 2016;37:104–12, <http://dx.doi.org/10.1002/adv.21646>.
- [30] Ilyas RA, Sapuan SM, Ishak MR, Zainudin ES. Sugar palm nanocrystalline cellulose reinforced sugar palm starch composite: degradation and water-barrier properties. *IOP Conf Series: Mater Sci Eng* 2018;368:012006, <http://dx.doi.org/10.1088/1757-899X/368/1/012006>.
- [31] Ilyas RA, Sapuan SM, Ishak MR, Zainudin ES. Sugar palm nanofibrillated cellulose (*Arenga pinnata* (Wurmb.) Merr): effect of cycles on their yield, physico-chemical, morphological and thermal behavior. *Int J Biol Macromol* 2019;123:379–88, <http://dx.doi.org/10.1016/j.ijbiomac.2018.11.124>.
- [32] Ilyas RA, Sapuan SM, Ibrahim R, Abrial H, Ishak MR, Zainudin ES, et al. Sugar palm (*Arenga pinnata* (Wurmb.) Merr) cellulosic fibre hierarchy: a comprehensive approach from macro to nano scale. *J Mater Res Technol* 2019, <http://dx.doi.org/10.1016/j.jmrt.2019.04.011>.